CHEMISTRY
A EUROPEAN JOURNAL

DOI: 10.1002/chem.200901842

A New Class of Modular P,N-Ligand Library for Asymmetric Pd-Catalyzed Allylic Substitution Reactions: A Study of the Key Pd–π-Allyl Intermediates

Javier Mazuela,[a] Alexander Paptchikhine,[b] Päivi Tolstoy,[b] Oscar Pàmies,[a] Montserrat Diéguez,*[a] and Pher G. Andersson*[b]

Abstract: A new class of modular P,N-ligand library has been synthesized and screened in the Pd-catalyzed allylic substitution reactions of several substrate types. These series of ligands can be prepared efficiently from easily accessible hydroxyl–oxazole/thiazole derivatives. Their modular nature enables the bridge length, the substituents at the heterocyclic ring and in the alkyl backbone chain, the configuration of the ligand backbone, and the substituents/configurations in the biaryl phosphite moiety to be easily and systematically varied. By carefully selecting the ligand components, therefore, high regio- and enantioselectivities (*ee* values up to 96%) and good activities are achieved in a broad range of mono-, di-, and trisubstituted linear hindered and unhindered substrates and cyclic substrates. The NMR spectroscopic and DFT studies on the Pd–π-allyl intermediates provide a deeper understanding of the effect of ligand parameters on the origin of enantioselectivity.

Keywords: allylic substitution · asymmetric catalysis · ligand design · N,P ligands · palladium

Introduction

The development of methods for enantioselective carbon–carbon and carbon–heteroatom bond formation is one of the key issues in organic synthesis. A versatile method for forming these bonds is palladium-catalyzed asymmetric allylic substitution.[1]

Most of the successful ligands reported to date for this process have been designed using three main strategies. The first one, developed by Hayashi and co-workers, was the use of a secondary interaction of the nucleophile with a side chain of the ligand to direct the approach of the nucleophile to one of the allylic terminal carbon atoms.[2] The second one, developed by Trost and co-workers, was to increase the bite angle of the ligand to create a chiral cavity in which the allyl system is embedded. This idea opened up the successful application of ligands with large bite angles for the allylic substitution of sterically undemanding substrates.[1,3] The third strategy, developed by groups led by Helmchen, Pfaltz, and Williams, was the use of heterodonor ligands that result in an electronic discrimination of the two allylic terminal carbon atoms due to the different *trans* influences of the donor groups.[1,4] This made it possible to successfully use a wide range of heterodonor ligands (mainly P,N ligands) in allylic substitution reactions.[1]

Nowadays, many chiral ligands (mainly P and N ligands), which possess either C_2 or C_1 symmetry, have been developed, and they provide high enantiomeric excesses for several types of disubstituted substrates.[1] Nevertheless, in general, there is still a problem of substrate specificity (for example, *ee* values are high in disubstituted linear hindered substrates and low in unhindered substrates, and vice versa) and reaction rates. Other types of substrates still require much attention. For example, for monosubstituted substrates, more active and more regio- and enantioselective Pd catalysts are needed.[1] Another challenging class of substrates is that of trisubstituted substrates. Although a few good enantioselective Pd-catalytic systems have been reported, their activities are still very low.[1] More research is needed on the development of new ligands that can overcome these limitations.

[a] J. Mazuela, Dr. O. Pàmies, Dr. M. Diéguez
Departament de Química Física i Inorgànica
Universitat Rovira i Virgili
C/Marcel líDomingo, s/n. 43007 Tarragona (Spain)
Fax: (+34) 977559563
E-mail: montserrat.dieguez@urv.cat

[b] A. Paptchikhine, P. Tolstoy, Prof. P. G. Andersson
Department of Biochemistry and Organic Chemistry
Uppsala University, BOX 576, 751 23 Uppsala (Sweden)
Fax: (+46) 18-471-3818
E-mail: pher.andersson@kemi.uu.se

Supporting information for this article is available on the WWW under http://dx.doi.org/10.1002/chem.200901842.

In this context, we recently demonstrated that the presence of biaryl phosphite moieties in ligand design is highly advantageous because 1) substrate specificity decreases because the chiral pocket created (i.e., the chiral cavity in which the allyl is embedded) is flexible enough to enable the perfect coordination of hindered and unhindered substrates,[5] 2) reaction rates increase thanks to the larger π-acceptor ability of these moieties,[6] and 3) regioselectivity towards the desired branched isomer in monosubstituted linear substrates increases, thanks to the π-acceptor ability of the phosphite moiety that enhances the S_N1 character of the nucleophilic attack.[7]

Due to our interest in discovering faster and more versatile Pd-catalytic systems, we decided to go one step further in the design of a new ligand library for this process. Therefore, we developed a ligand library, the design of which incorporates the advantages of heterodonor and biaryl phosphite ligands and also allows extra control of the flexibility of the chiral pocket by changing the size of the chelate ring. To do this, we synthesized and screened a library of 56 potential new phosphite–oxazole/thiazole ligands.[8] The highly modular construction of these ligands enabled a systematic study of the effect of bridge length (ligands **L1** and **L6**), the substituent at the heterocyclic ring (ligands **L1**–**L4**) and in the alkyl backbone chain (ligands **L6** and **L7**), the configuration of the ligand backbone (ligands **L1** vs. **L5** and **L7** vs. **L8**), and the substituents and configurations in the biaryl phosphite moiety (**a**–**g**). By carefully selecting these elements, we achieved high selectivities (regio- and enantioselectivities) and activities in a wide range of mono-, di-, and trisubstituted substrates. In this paper we also discuss the synthesis and characterization of the Pd–π-allyl intermediates to provide greater insight into the origin of enantioselectivity in these catalytic systems.

Results and Discussion

Synthesis of the ligand library: Scheme 1 illustrates the sequence of ligand synthesis. Ligands **L1**–**L8a**–**g** were synthesized very efficiently from the corresponding easily accessible ketone–oxazole or thiazole–ester derivatives (**2**–**5** and **12**, Scheme 1). Compounds **2**–**5** and **12** are easily made in two steps from the corresponding dimedone **1** and ketoester **11**, respectively (see the Experimental Section).[9] Ketone–oxazoles **2**–**5** were then reduced using (*R*)-Me-CBS or $NaBH_4$ (CBS = oxazaborolidine; Scheme 1, step b). Enantioselective reduction of **2** using (*R*)-Me-CBS followed by single recrystallization afforded hydroxyl–oxazole **6** in >99% *ee*.[9a] The same procedure applied to ketones **3** and **4** afforded hydroxyl–oxazoles **8** and **9** but with *ee* values of <80%. Thus, further enantiomer resolution was achieved using preparative chiral HPLC. For compounds **7** and **10**, the corresponding ketone–oxazoles **2** and **5** were reduced using $NaBH_4$ followed by enantiomer resolution using preparative HPLC. Reduction of **12** using $LiAlH_4$ (Scheme 1, step d)[9b] or MeMgCl (Scheme 1, step e) gave good yields of the corresponding racemic alcohols **13** and **14**, respectively. This was followed by the resolution of racemates into their enantiomers by preparative chiral HPLC.[9]

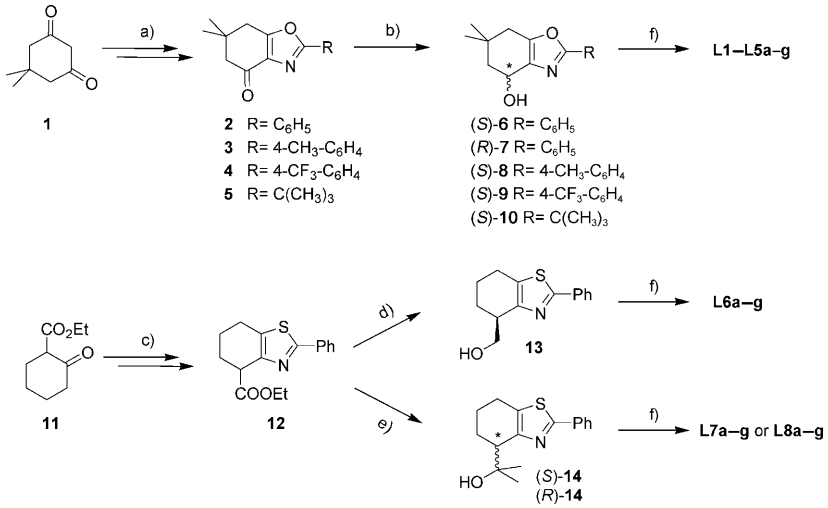

Scheme 1. Synthesis of a new phosphite–nitrogen ligand library **L1**–**L8a**–**g**. a), b) see ref. [9a] and the Experimental Section; c), d) see ref. [9b]; e) $CH_3MgCl/THF/CeCl_3$ (yield: 71%); f) $ClP(OR)_2$; $(OR)_2$ = **a**–**g**/pyridine/toluene (yields: 42–76%).

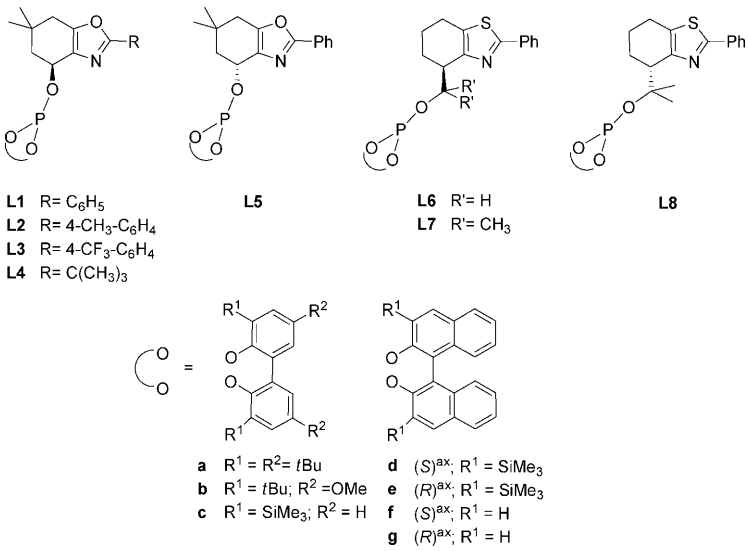

The last step of the ligand synthesis is common to all of them (Scheme 1, step f). Therefore, treatment of the corresponding hydroxyl–oxazole (**6**–**10**) or hydroxyl–thiazole (**13** and **14**) with 1 equiv of the corresponding in situ formed biaryl phosphorochloridite ($ClP(OR)_2$; $(OR)_2$ = **a**–**g**) in the presence of pyridine, in a parallel manner, provided easy access to the desired ligands **L1**–**L8 a**–**g** (see the Experimental Section for details). All of the ligands were stable during purification on neutral alumina under an atmosphere of argon and isolated in moderate-to-good yields as white solids. They were stable at room temperature and very stable to hydrolysis. The elemental analyses were in agreement with the assigned structure. The ^{1}H, ^{13}C, and ^{31}P NMR spectra were as expected for these C_1 ligands. One singlet for each compound was observed in the ^{31}P NMR spectrum (see the Experimental Section). Rapid ring inversions (atropoisomerization) in the biphenylphosphorus moieties (**a**–**c**) occurred on the NMR spectroscopic timescale because the expected diastereoisomers were not detected by low-temperature phosphorus NMR spectroscopy.[10]

Allylic substitution of symmetrical 1,3-disubstituted allylic substrates: In this section, we report the use of the chiral phosphite–nitrogen ligand library (**L1**–**L8 a**–**g**) in the Pd-catalyzed allylic substitution of linear disubstituted substrates with different steric properties [Eq. (1 a)]: *rac*-1,3-diphenyl-3-acetoxyprop-1-ene (**S1**) (widely used as a model substrate), *rac*-(*E*)-ethyl-2,5-dimethyl-3-hex-4-enylcarbonate (**S2**), and *rac*-1,3-dimethyl-3-acetoxyprop-1-ene (**S3**); and cyclic substrates [Eq. (1 b)]: *rac*-3-acetoxycyclohexene (**S4**) (widely used as a model substrate), *rac*-3-acetoxycycloheptene (**S5**), and *rac*-3-acetoxycyclopentene (**S6**). Two nucleophiles were tested. In all cases, the catalysts were generated in situ from π-allyl–palladium chloride dimer [{$PdCl(\eta^3$-$C_3H_5)$}$_2$] and the corresponding ligand.[1]

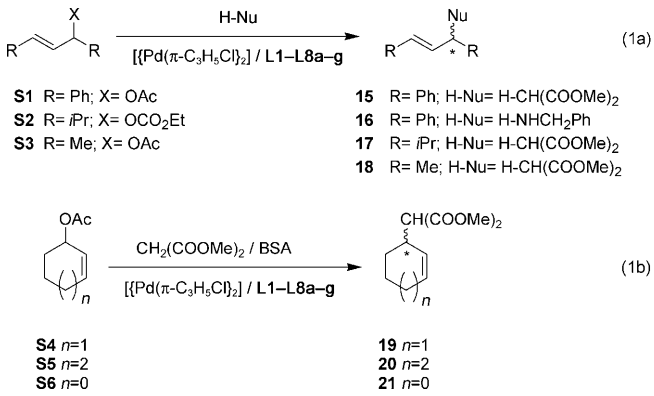

Allylic substitution of S1 using dimethyl malonate and benzylamine as nucleophiles: In the first set of experiments, we used the palladium-catalyzed asymmetric substitution reactions of **S1** [Eq. (1 a); R = Ph, X = OAc], with dimethyl malonate and benzylamine as nucleophiles, to study the potential of the phosphite–nitrogen ligand library **L1**–**L8 a**–**g**. Compound **S1** was chosen as a substrate because the reaction was performed with a wide range of ligands, which enabled the efficiency of the various ligand systems to be compared directly.[1]

First, we studied the effect of the reaction conditions by conducting a series of experiments with two ligands (**L1 a** and **L6 a**) using different solvents (tetrahydrofuran, toluene, and dichloromethane) and ligand-to-palladium ratios (L/Pd = 0.75, L/Pd = 1, and L/Pd = 2). We found that the efficiency of the process was strongly dependent on the nature of the solvent and the ligand-to-palladium ratio (Table 1).

Table 1. Selected results for the Pd-catalyzed allylic alkylation of **S10** by using ligand library **L1**–**L8 a**–**g**. Effects of the solvent and the ligand-to-palladium ratio.[a]

Entry	Ligand	Solvent	L/Pd	Conv [%] (*t* [min])[b]	*ee* [%][c]
1	**L1 a**	CH_2Cl_2	1	100 (30)	82 (*S*)
2	**L1 a**	THF	1	89 (60)	73 (*S*)
3	**L1 a**	toluene	1	100 (1440)	92 (*S*)
4	**L6 a**	CH_2Cl_2	1	100 (30)	21 (*S*)
5	**L6 a**	THF	1	85 (180)	18 (*S*)
6	**L6 a**	toluene	1	64 (600)	34 (*S*)
7	**L1 a**	CH_2Cl_2	0.75	100 (60)	82 (*S*)
8	**L6 a**	CH_2Cl_2	2	100 (30)	79 (*S*)
9	**L6 a**	CH_2Cl_2	0.75	73 (30)	23 (*S*)
10	**L6 a**	CH_2Cl_2	2	100 (30)	14 (*S*)

[a] All reactions were run at 23 °C; 0.5 mol % [{$PdCl(\eta^3$-$C_3H_5)$}$_2$]; **S1** (0.5 mmol); BSA (*N*,*O*-bis(trimethylsilyl)acetamide) (1.5 mmol); dimethyl malonate (1.5 mmol). [b] Conversion measured by ^{1}H NMR spectroscopy. Reaction time shown in parentheses. [c] Enantiomeric excesses measured by HPLC. Absolute configuration shown in parentheses.

Although in toluene the enantioselectivity was higher than dichloromethane, the activity was much lower (Table 1, entries 3 and 6 vs. entries 1 and 4). Tetrahydrofuran yielded the lowest enantioselectivities of all three solvents (entries 2 and 5). We also found that an excess of ligand was not needed for enantioselectivities to be high (entries 1, 4, and 7–10). Interestingly, at higher ligand-to-palladium ratios, enantioselectivities were lower (entries 8 and 10 vs. entries 1 and 4). This is probably due to the fact that at a ligand-to-palladium ratio greater than 1, the phosphite–nitrogen ligands act as a monodentate ligand.[11]

For comparison purposes, the rest of the ligands were tested using dichloromethane as a solvent and at a ligand-to-palladium ratio of 1. Table 2 shows the results obtained when dimethyl malonate and benzylamine were used as nucleophiles. We found that enantioselectivities were highly affected by the bridge length, the substituents at the heterocyclic ring and in the alkyl backbone chain, and the substituents and configurations in the biaryl phosphite moieties (**a**–**g**). High activities (turnover frequencies (TOFs) up to 600 mol **S1** × (mol Pd × h)$^{-1}$) and enantioselectivities (*ee* values up to 92 %) were obtained for both enantiomers of the substitution products **15** and **16** using ligands **L1 a** and **L5 a**. Catalytic performance in the Pd-catalyzed allylic ami-

Table 2. Selected results for the Pd-catalyzed allylic substitution of **S1** by using ligand library **L1–L8a–g**.[a]

		H–Nu = H–CH(COOMe)$_2$[a]		H–Nu = H–NHCH$_2$Ph[a]	
Entry	Ligand	Conv [%] (t [min])[b]	*ee* [%][c]	Conv [%] (t [min])[b]	*ee* [%][c]
1	**L1a**	100 (15)[d]	82 (*S*)	34 (360)	84 (*R*)
2	**L1b**	99 (20)	81 (*S*)	37 (360)	80 (*R*)
3	**L1c**	99 (15)	70 (*S*)	43 (360)	69 (*R*)
4	**L1d**	100 (30)[d]	69 (*S*)	28 (360)	71 (*R*)
5	**L1e**	100 (30)[d]	40 (*S*)	31 (360)	41 (*R*)
6	**L1f**	72 (30)	9 (*S*)	15 (360)	7 (*R*)
7	**L1g**	42 (30)	8 (*R*)	12 (360)	5 (*S*)
8	**L2a**	80 (30)	43 (*S*)	24 (360)	32 (*R*)
9	**L3a**	98 (30)[d]	79 (*S*)	36 (360)	82 (*R*)
10	**L4a**	78 (30)	22 (*S*)	19 (360)	25 (*R*)
11	**L5a**	100 (15)	81 (*R*)	32 (360)	84 (*S*)
12	**L6a**	100 (20)[d]	21 (*S*)	41 (360)	19 (*R*)
13	**L7a**	100 (30)[d]	52 (*S*)	38 (360)	49 (*R*)
14	**L8a**	100 (30)	51 (*R*)	33 (360)	50 (*S*)
15[e]	**L1a**	100 (360)	92 (*S*)	–	–

[a] All reactions were run at 23 °C; 0.5 mol % [{PdCl(η^3-C$_3$H$_5$)}$_2$]; dichloromethane as solvent; 1 mol % ligand. [b] Conversion measured by ^{1}H NMR spectroscopy. Reaction time shown in parentheses. [c] Enantiomeric excesses measured by HPLC. Absolute configuration shown in parentheses. [d] Isolated yields of **15** were >93 %. [e] Toluene as solvent.

nation of **S1** followed the same trend as for the allylic alkylation of **S1** (Table 2). As expected, however, the activity was lower than in the alkylation reaction of **S1**. The stereoselectivity of the amination was the same as for the alkylation reaction, though the Cahn–Ingold–Prelog (CIP) descriptor was inverted because the priority of the groups had changed.

The influence of the bridge length indicates that the use of ligands **L1** and **L5**, which form a six-membered chelate ring, provided higher enantioselectivity than the use of ligands **L6–L8**, which form a seven-membered chelate ring (Table 2, entries 1 and 11 vs. entries 12–14). In line with this, the increase of the rigidity of the ligand by replacing the hydrogen substituents in the alkyl backbone chain in ligand **L6a** with two methyl groups (ligand **L7a**) caused enantioselectivities to increase (Table 2, entries 12 vs. 13).

The effect of the substituents at the heterocyclic ring indicated that the presence of either bulky or electron-donating substituents decreased both activities and enantioselectivities (Table 2, entries 1, 8–10). The fact that enantiomeric excesses decrease when a bulky *tert*-butyl is present is due to the formation of Pd intermediate species with the phosphite–nitrogen ligand acting as a monodentate ligand (see below).

Regarding the effect of the substituents at the biphenyl phosphite moiety, we found that the presence of bulky *tert*-butyl substituents at both the *ortho* and *para* positions is highly adventitious in terms of activity and enantioselectivity (Table 2, entry 1). Therefore, the presence of methoxy groups in the *para* position of the biphenyl moieties has a negative effect on activity, whereas the presence of trimethylsilyl substituents at the *ortho* positions has a negative effect on enantioselectivity (Table 2, entries 2 and 3 vs. entry 1). With ligands **L1d** and **L1e**, which contain different enantiomerically pure binaphthyl moieties, we found that there is a cooperative effect between the configuration of the biaryl moiety and the configuration of the ligand backbone on enantioselectivity. This led to a matched combination for ligand **L1d**, which contains an (*S*)-binaphthyl moiety (Table 2, entries 4 and 5). In addition, by comparing the results obtained using ligand **L1c** with those of the related binaphthyl ligands **L1d** and **L1e** (Table 2, entries 3–5), we can also conclude that the atropoisomeric biphenyl moiety in ligands **L1a–c** adopts an *S* configuration when coordinated in the Pd–π-allyl intermediate species.

To sum up, the best result was obtained with ligands **L1a** and **L5a**, which contain the optimal combination of ligand parameters (Table 2, entries 1 and 11). These findings clearly show the efficiency of highly modular scaffolds in ligand design. Enantioselectivity can be further improved by controlling not only the structural but also the reaction parameters. As expected, changing the solvent from dichloromethane to toluene increased enantioselectivity (*ee* values up to 92 %, Table 2, entry 15).

Allylic substitution of S2 using dimethyl malonate as nucleophile: We also screened the phosphite–nitrogen ligand library **L1–L8a–g** in the allylic alkylation process of **S2** using dimethyl malonate as nucleophile [Eq. (1a); R = *i*Pr, X = OCO$_2$Et]. This substrate is more sterically demanding than substrate **S1**, which was used previously.[1] If enantiomeric excesses are to be high, the ligand must create a slightly bigger chiral pocket (the chiral cavity in which the allyl is embedded) around the metal center to be able to accommodate the sterically demanding isopropyl substituents.[1] Due to the flexibility conferred by the biaryl phosphite moiety, we expected to obtain good enantioselectivities for this substrate as well. Table 3 shows the most representative results. In general, the trends were the same as for the allylic substitution of **S1**. Again, both enantiomers of the alkylation product **17** were accessible in high enantioselectivities (*ee* values up to 93 %) when catalyst precursors containing ligands **L1a** and **L5a** were used (Table 3, entries 1, 9, 13, and 14). As expected, the activities were lower than in the alkylation reaction of **S1**.[1] The stereoselectivity of the alkylation of **S2** was the same as for the alkylation reaction of **S1**, though the CIP descriptor was inverted because of the change in the priority of the groups.

Allylic substitution of S3 using dimethyl malonate as nucleophile: We also tested ligands **L1–L8a–g** in the allylic substitution of the linear substrate **S3** [Eq. (1a); R = Me, X = OAc]. Substrate **S3** is less sterically demanding than sub-

Table 3. Selected results for the Pd-catalyzed allylic substitution of **S2** by using ligand library **L1–L8 a–g**.[a]

Entry	Ligand	Conv [%] (t [h])[b]	ee [%][c]
1[d]	**L1 a**	100 (24)	84 (R)
2	**L1 b**	95 (24)	82 (R)
3	**L1 c**	100 (24)	73 (R)
4	**L1 d**	78 (24)	67 (R)
5	**L1 e**	82 (24)	39 (R)
6	**L2 a**	75 (24)	47 (R)
7[d]	**L3 a**	100 (24)	77 (R)
8	**L4 a**	69 (24)	60 (R)
9	**L5 a**	100 (24)	83 (S)
10[d]	**L6 a**	100 (24)	12 (R)
11	**L7 a**	100 (24)	24 (R)
12	**L8 a**	100 (24)	23 (S)
13[e]	**L1 a**	99 (48)	93 (R)
14[e]	**L5 a**	94 (48)	92 (S)

[a] All reactions were run at 23 °C; 1 mol % [{PdCl(η^3-C_3H_5)}$_2$]; dichloromethane as solvent; 2 mol % ligand. [b] Conversion measured by ^{1}H NMR spectroscopy. Reaction time shown in parentheses. [c] Enantiomeric excesses measured by ^{1}H NMR spectroscopy using [Eu(hfc)$_3$]. Absolute configuration shown in parentheses. [d] Isolated yields of **17** were >92 %. [e] Toluene as solvent.

Table 4. Selected results for the Pd-catalyzed allylic substitution of **S3** by using ligand library **L1–L8 a–g**.[a]

Entry	Ligand	Conv [%] (t [h])[b]	ee [%][c]
1[d]	**L1 a**	100 (1)	59 (S)
2	**L1 b**	100 (1)	67 (S)
3	**L1 c**	100 (1)	54 (S)
4[d]	**L1 d**	100 (2)	75 (S)
5[d]	**L1 e**	100 (2)	51 (S)
6	**L1 f**	82 (2)	30 (S)
7	**L1 g**	63 (2)	21 (S)
8[d]	**L2 a**	100 (2)	60 (S)
9[d]	**L2 e**	100 (2)	74 (S)
10[d]	**L3 a**	100 (2)	59 (S)
11[d]	**L3 e**	100 (2)	75 (S)
12[d]	**L4 a**	100 (2)	5 (S)
13	**L5 a**	100 (1)	57 (R)
14	**L6 a**	92 (2)	38 (S)
15	**L7 a**	93 (3)	80 (S)
16	**L7 d**	100 (4)	87 (S)
17	**L8 d**	100 (4)	87 (R)
18[d,e]	**L1 d**	100 (20)	84 (S)
19[e]	**L7 d**	96 (24)	92 (S)

[a] All reactions were run at 23 °C; 0.5 mol % [{PdCl(η^3-C_3H_5)}$_2$]; dichloromethane as solvent; 1 mol % ligand. [b] Conversion measured by GC. Reaction time shown in parentheses. [c] Enantiomeric excesses measured by GC. Absolute configuration shown in parentheses. [d] Isolated yields of **18** were >91 %. [e] T = 0 °C.

strates **S1** and **S2**, used previously. There are therefore fewer successful catalyst systems for the Pd-catalyzed allylic substitution of this substrate than for the allylic substitution of hindered substrates such as **S1** and **S2**.[3b,5,6e,11b,12] If enantiomeric excesses are to be high, the ligand must create a small chiral pocket around the metal center, mainly because of the presence of less sterically demanding methyl *syn* substituents.[1] Due to the flexibility conferred by the biaryl phosphite moiety in combination with the possibility of changing the size of the chelate ring in the ligand, we expected to adequately modulate the chiral pocket to obtain good enantioselectivities for this substrate as well.

Preliminary investigations into the solvent and ligand-to-palladium ratio revealed a different trend in solvent effect than with the previously tested substrates **S1** and **S2**. Enantioselectivities and activities were both at their highest when dichloromethane was used and the ligand-to-palladium ratio was 1 (see the Supporting Information).

Table 4 shows the results obtained using the ligand library **L1–L8 a–g** in optimized conditions. We were able to fine-tune the ligands to obtain high activities and enantioselectivities (ee values up to 92 %) in the alkylation of this substrate. Again, activities and enantioselectivities were affected by the bridge length, the substituent at the nitrogen heterocycle, and the substituents and configurations in the biaryl phosphite moiety. However, the effect of these parameters was different from their effect on substitution of hindered substrates **S1** and **S2**. Enantioselectivities were best with ligands **L7 d** and **L8 d** (Table 4, entries 16, 17, and 19). Once again, it was possible to access both enantiomers of the substitution product **18**. These results, which again clearly show the efficiency of using modular scaffolds in ligand design, are among the best reported for this type of unhindered substrate.[3b,5,6e,11b,12]

Regarding the effect of ligand flexibility, in contrast to **S1** and **S2**, the highest enantioselectivities were obtained with ligands **L7** and **L8**, which form a seven-membered chelate ring and contain two methyl groups at the alkyl backbone chain. Concerning the effect of the substituents at the heterocyclic ring and the biaryl phosphite moiety, in contrast to **S1** and **S2**, the presence of aryl substituents in the heterocyclic moiety and a bulky (S)-binaphthyl phosphite moiety had a positive effect on enantioselectivities. In conclusion, our results indicate that both the size of the chelate ring and the flexibility of the biaryl phosphite moiety are the main ligand parameters that control the size of the chiral pocket to achieve high enantioselectivities.

Allylic alkylation of cyclic substrates S4–S6: With the unhindered cyclic substrates **S4–S6**, enantioselectivity is difficult to control, mainly because of the presence of less sterically demanding *anti* substituents. These *anti* substituents are thought to play a crucial role in the enantioselection observed with cyclic substrates in the corresponding Pd–allyl intermediates.[1]

In this section, we show that the chiral ligand library **L1–L8 a–g** that was applied previously to the Pd-catalyzed allylic substitution of 1,3-disubstituted linear substrates (**S1–S3**) can also be used for cyclic substrates (ee values up to 88 %). We tested three cyclic substrates [Eq. (1 b)]: *rac*-3-acetoxycyclohexene (**S4**) (which is widely used as a model substrate), *rac*-3-acetoxycycloheptene (**S5**), and *rac*-3-acetoxycyclopentene (**S6**).

Preliminary investigations into the solvent effect and ligand-to-palladium ratio showed the same trends as with the previously tested unhindered linear substrate **S3**. The

tradeoff between enantioselectivities and reaction rates was therefore optimum with dichloromethane and a ligand-to-palladium ratio of 1 (see the Supporting Information).

Table 5 shows the results of using the ligand library **L1**–**L8a–g** under the optimized conditions. We also obtained high activities and enantioselectivities (up to 88%) in the allylic substitution of the cyclic substrates **S4**–**S6** using ligands **L1d**, **L1e**, and **L3e**. The results indicate that the effect of the ligand parameters on the catalytic performance are different from those observed for the linear substrates **S1**–**S3**. In contrast to the alkylation of unhindered linear **S3**, ligands that form a six-membered chelate ring (**L1**) provided higher enantioselectivities than those that form a seven-membered chelate ring (**L6**, **L7**). The results also indicate that the presence of an enantiopure bulky binaphthyl phosphite moiety (**d** and **e**) is therefore required for enantioselectivity to be high (Table 5, entries 4, 5, 8, 14, and 15). Interestingly, the sense of enantioselectivity is also governed by the configuration of the biaryl phosphite moiety. Thus, both enantiomers of the substitution products **19**–**21** can be accessed in high enantioselectivities by simply changing the configuration of the trimethylsilyl-substituted binaphthyl moiety (Table 5, entries 4 and 5).

Table 5. Selected results for the Pd-catalyzed allylic substitution of **S4**–**S6** by using ligand library **L1**–**L8a–g**.[a]

Entry	Substrate	Ligand	Conv [%] (t [h])[b]	ee [%][c]
1	**S4**	**L1a**	100 (6)	41 (S)
2	**S4**	**L1b**	100 (6)	59 (S)
3	**S4**	**L1c**	100 (6)	43 (S)
4[d]	**S4**	**L1d**	100 (6)	80 (S)
5[d]	**S4**	**L1e**	100 (6)	85 (R)
6	**S4**	**L2a**	100 (6)	41 (S)
7	**S4**	**L3a**	100 (6)	45 (S)
8[d]	**S4**	**L3e**	100 (6)	84 (R)
9[d]	**S4**	**L4a**	100 (6)	60 (S)
10	**S4**	**L5a**	100 (6)	39 (R)
11	**S4**	**L6a**	100 (6)	13 (S)
12	**S4**	**L7a**	100 (6)	29 (S)
13	**S4**	**L7d**	100 (6)	63 (S)
14	**S5**	**L1d**	100 (24)	83 (S)
15[d]	**S5**	**L1e**	100 (24)	88 (R)
16	**S6**	**L1d**	100 (6)	72 (S)
17	**S6**	**L1e**	100 (6)	71 (R)

[a] All reactions were run at 23°C; 0.5 mol% $[\{PdCl(\eta^3\text{-}C_3H_5)\}_2]$; dichloromethane as solvent; 1 mol% ligand. [b] Conversion measured by GC. Reaction time shown in parentheses. [c] Enantiomeric excesses measured by GC. Absolute configuration shown in parentheses. [d] Isolated yields of **19** and **20** were >91%.

In summary, the enantioselectivities obtained with ligands **L1d**, **L1e**, and **L3e** are among the best reported for this type of 1,3-disubstituted cyclic substrate.[1e,3a,5a,11b,12a,13] Interestingly, compared with the hindered substrates **S1** and **S2** and in contrast to the unhindered linear substrate **S3**, the flexibility conferred by the biaryl phosphite moiety was enough to adequately control the size of the chiral pocket to achieve high enantioselectivities.

Allylic substitution of unsymmetrical 1,3,3-trisubstituted allylic substrate: We also screened the ligands **L1**–**L8a–g** in the allylic substitution of *rac*-1,3,3-triphenylprop-2-enyl acetate (**S7**) and *rac*-1,1-diphenyl-1-hepten-3-yl acetate (**S8**) using dimethylmalonate as nucleophile [Eq. (2); R = R′ = R″ = Ph for **S7** and R = R′ = Ph, R″ = Me for **S8**]. These substrates are of synthetic interest because the substitution products formed in this way can easily be transformed into enantiomerically enriched acid derivatives and lactones.[14] They are more sterically demanding than the previously used substrate **S1**,[1] and it is therefore more difficult to achieve excellent enantioselectivities with them than with **S1**.[12,15] Interestingly, with this P,N-ligand library, we obtained high enantiomeric excesses (ee values up to 96%) under standard reaction conditions. Although, as expected, the activities were lower than in the alkylation reaction of **S1**, they were much higher than those obtained with other successful ligands under similar reaction conditions.[15]

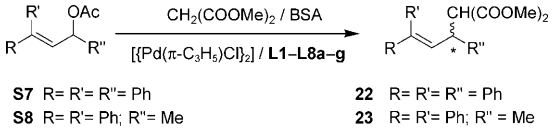

The results, summarized in Table 6, followed a trend similar to that of the more hindered substrates **S1** and **S2**. Thus, ligands **L1** and **L5**, which form a six-membered chelate ring and have a phenyl substituent at the nitrogen heterocycle, provided better enantioselectivities than ligands **L2**–**L4** and **L6**–**L8**. The presence of bulky substituents at the *ortho* positions of the biaryl phosphite moiety was necessary for enantioselectivities to be high. However, in contrast to **S1** and **S2**, enantioselectivities were less affected by the presence or lack of bulky substituents at the *para* positions of the biaryl phosphite moiety. Therefore, ligands **L1a–c** and **L5a–c** pro-

Table 6. Selected results for the Pd-catalyzed allylic substitution of **S7** and **S8** by using ligand library **L1**–**L8a–g**.[a]

Entry	Ligand	**S7** Conv [%] (t [h])[b]	ee [%][c]	**S8** Conv [%] (t [h])[b]	ee [%][c]
1[d]	**L1a**	92 (24)	88 (R)	100 (24)	95 (R)
2	**L1b**	88 (24)	95 (R)	100 (24)	94 (R)
3	**L1c**	79 (24)	96 (R)	100 (24)	95 (R)
4	**L1d**	46 (24)	42 (R)	53 (24)	32 (R)
5	**L1g**	33 (24)	18 (R)	48 (24)	21 (R)
6	**L2a**	90 (24)	81 (R)	100 (24)	78 (R)
7	**L3a**	88 (24)	90 (R)	100 (24)	85 (R)
8	**L4a**	45 (24)	23 (R)	85 (24)	38 (R)
9	**L5a**	88 (24)	90 (S)	100 (24)	95 (S)
10	**L6a**	67 (24)	40 (R)	73 (24)	57 (R)
11	**L7a**	29 (24)	30 (R)	46 (24)	44 (R)
12	**L8a**	27 (24)	30 (S)	42 (24)	42 (S)

[a] All reactions were run at 23°C; 1 mol% $[\{PdCl(\eta^3\text{-}C_3H_5)\}_2]$; dichloromethane as solvent; 2 mol% ligand. [b] Conversion measured by ^{1}H NMR spectroscopy. Reaction time shown in parentheses. [c] Enantiomeric excesses measured by ^{1}H NMR spectroscopy. Absolute configuration shown in parentheses. [d] Isolated yields of **22** and **23** were >88%.

vided excellent enantiocontrol in the allylic substitution of the trisubstituted substrates **S7** and **S8**, and also gave access to both enantiomers of the alkylation products **22** and **23** (*ee* values up to 96%). These results are among the best reported for this class of substrate.[15]

Allylic substitution of unsymmetrical 1- or 3-monosubstituted allylic substrates: To further study the potential of these readily available ligands, we tested **L1–L8a–g** in the regio- and stereoselective allylic alkylation of 1-(1-naphthyl)allyl acetate (**S9**) and 1-(1-naphthyl)-3-acetoxyprop-1-ene (**S10**) with dimethyl malonate as nucleophile [Eq. (3)].

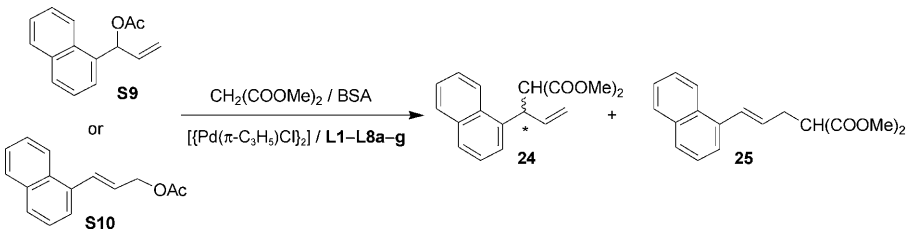

(3)

For these substrates, not only does the enantioselectivity of the process need to be controlled but regioselectivity is also a problem because a mixture of regioisomers can be obtained. Most Pd catalysts developed to date favor the formation of achiral linear product **25** rather than the desired branched isomer **24**.[16] The development of highly regio- and enantioselective Pd catalysts is therefore still important.[5a,7,11b,17]

Table 7 summarizes the results obtained with the ligand library **L1–L8a–g**. High activities and enantioselectivities (of up to 92%) combined with regioselectivities of up to 80% in favor of the branched product **24** were obtained under standard reaction conditions. The results indicate that the selectivity (regio- and enantioselectivity) is mainly affected by the ligand backbone, the substituent at the nitrogen heterocycle, and the substituents and configurations in the biaryl phosphite moiety. However, no general trend was seen. The tradeoff between regio- and enantioselectivities was best for ligand **L7a**, which forms a seven-membered chelate ring and has methyl substitutents at the alkyl-backbone chain and bulky *tert*-butyl groups at the *ortho* and *para* positions of the biphenyl phosphite moiety (Table 7, entries 14 and 19). Again, these results are among the best reported for this type of substrate.[5a,7,11b,17]

Table 7. Selected results for the Pd-catalyzed allylic alkylation of monosubstituted substrates **S9** and **S10** by using ligand library **L1–L8a–g** under standard conditions.[a]

Entry	Ligand	Substrate	Conv [%] (t [min])[b]	**24/25**[c]	*ee* [%][d]
1	**L1a**	**S9**	100 (30)	70:30	20 (*R*)
2	**L1b**	**S9**	100 (30)	40:60	63 (*R*)
3	**L1c**	**S9**	100 (30)	55:45	70 (*R*)
4	**L1d**	**S9**	100 (30)	50:50	78 (*R*)
5	**L1e**	**S9**	100 (30)	55:45	34 (*R*)
6[e]	**L2a**	**S9**	100 (30)	80:20	45 (*R*)
7	**L2d**	**S9**	100 (30)	75:25	88 (*R*)
8	**L3a**	**S9**	100 (30)	75:25	19 (*R*)
9	**L3c**	**S9**	100 (30)	70:30	73 (*R*)
10	**L4a**	**S9**	100 (30)	75:25	25 (*R*)
11	**L6a**	**S9**	100 (30)	45:55	2 (*S*)
14	**L7a**	**S9**	100 (30)	80:20	92 (*R*)
15	**L7d**	**S9**	100 (30)	60:40	90 (*R*)
16	**L1d**	**S10**	100 (30)	50:50	79 (*R*)
17	**L3c**	**S10**	100 (30)	70:30	72 (*R*)
18	**L2d**	**S10**	100 (30)	75:25	87 (*R*)
19	**L7a**	**S10**	100 (30)	80:20	92 (*R*)

[a] All reactions were run at 23°C; 1 mol% [{PdCl((η^3-C_3H_5)}$_2$]; dichloromethane as solvent; 2 mol% ligand; substrate (0.5 mmol); BSA (1.5 mmol); dimethyl malonate (1.5 mmol). [b] Reaction time in minutes shown in parentheses. [c] Percentage of branched (**24**) and linear (**25**) isomers. [d] Enantiomeric excesses of **24** determined by HPLC. Absolute configuration shown in parentheses. [e] Isolated yield of **24** was >72%.

Origin of enantioselectivity—study of the Pd–π-allyl intermediates: To provide further insight into how ligand parameters affect catalytic performance, we studied the Pd–π-allyl compounds **26–35** [Pd(η^3-allyl)(L)]BF_4 (L = **L1–L8a–g**), because they are key intermediates in the allylic substitution reactions studied.[1] These ionic palladium complexes, which contain 1,3-diphenyl-, 1,3-dimethyl-, or cyclohexenylallyl groups, were prepared using the previously reported method from the corresponding Pd–allyl dimer and the appropriate ligand in the presence of silver tetrafluoroborate (Scheme 2).[18] The complexes were characterized by elemental analysis and by ^{1}H, ^{13}C, and ^{31}P NMR spectroscopy. The spectral assignments (see the Experimental Section) were based on information from ^{1}H,^{1}H, ^{31}P,^{1}H and ^{13}C,^{1}H correlation measurements in combination with ^{1}H,^{1}H NOESY experiments. Unfortunately, we were unable to obtain crystals of sufficient quality to perform X-ray diffraction measurements. For some of the key Pd–allyl complexes, we also performed a DFT study.

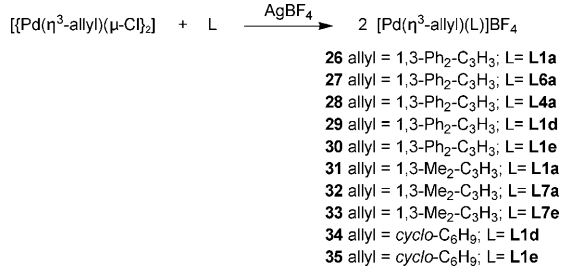

Scheme 2. Preparation of [Pd(η^3-allyl)(L)]BF_4 complexes **26–35**.

Palladium 1,3-diphenylallyl complexes: When the phosphite–nitrogen ligand library **L1–L8a–g** was used in the allylic substitution of substrate **S1**, the catalytic results showed that enantioselectivity is highly affected by the ligand pa-

rameters. A six-membered chelate ring, phenyl substituents in the nitrogen heterocyclic ring, and bulky substituents at the *ortho* position of the biaryl moiety are therefore required if enantioselectivity is to be high. To understand this catalytic behavior, we studied the Pd–π-allyl complexes **26**–**28**, which contain ligands **L1a**, **L6a**, and **L4a**, respectively. Finally, with complexes **29** and **30**, which contain ligands **L1d** and **L1e**, we studied the cooperative effect seen between the configuration of the ligand backbone and the configuration of the biaryl phosphite moiety.

The variable temperature (VT) NMR (30 to −80 °C) spectroscopic study of the Pd–allyl intermediate **26**, which contains ligand **L1a**, had a mixture of two isomers in equilibrium at a ratio of 9:1 (see the Experimental Section).[19] Both isomers were unambiguously assigned by NMR spectroscopy (^{1}H, ^{31}P, ^{13}C, ^{1}H,^{1}H, ^{1}H,^{13}C, and ^{1}H,^{31}P correlation and NOESY experiments) to the two *syn*/*syn endo* **A** and *exo* **B** isomers (Scheme 3). In both isomers, the NOE indicated interactions between the two terminal protons of the allyl group and also between the central allyl proton and *ortho*-hydrogen atoms of both phenyl groups of the allyl ligand, which clearly indicates a *syn*/*syn* disposition (Figure 1). Moreover, the central allyl proton showed a NOE interaction with the hydrogen of the CH−O group of the ligand backbone of the major isomer **A**, whereas in isomer **B** this interaction appeared with the hydrogen atoms of one *tert*-butyl group. These interactions can be explained by assuming a *syn*/*syn endo* disposition for isomer **A** and a *syn*/*syn exo* disposition for isomer **B** (Figure 1). We also carried out theoretical calculations at the DFT level for both isomers. Figure 1 shows these calculated structures and the relative values of the formation enthalpy, with isomer **A** being the most stable. The difference in the calculated formation enthalpy for the two isomers ($\Delta H = 1.8$ kcal mol^{-1}) is in agreement with the population observed by NMR spectroscopy of the different Pd-allyl intermediates formed in solution. For both isomers, the carbon NMR spectroscopic chemical shifts indicate that the more electrophilic allyl carbon terminus is *trans* to the phosphite moiety (Scheme 3). Assuming that the nucleophilic attack takes place at the more electrophilic allyl carbon terminus,[1] the matching between enantiomeric excesses (82 % *S* in product **15**) and the diastereoisomeric Pd ratio ($de = 80$ % (*S*)) indicate that the two isomers react at a similar rate. This is in agreement with the fact that the electrophilicities of the allylic terminal carbon atom *trans* to the phosphite are rather similar in both complexes ($\Delta(\delta^{13}C) = 0.5$ ppm). To prove this, we studied the reactivity of the Pd intermediates with sodium malonate at low temperature by in situ NMR spectroscopy (see the Supporting Information). Our results showed that the two isomers react at a similar rate.

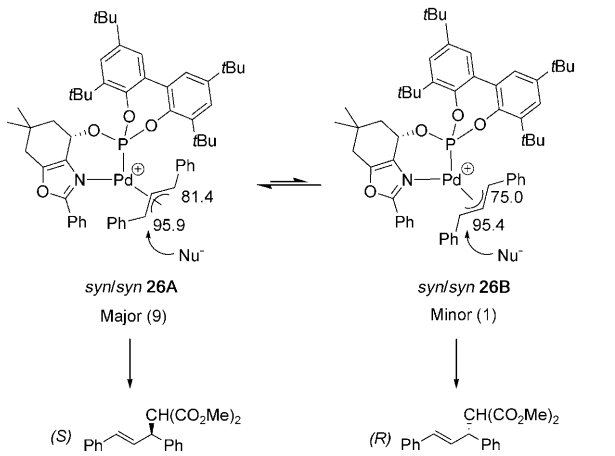

Scheme 3. Diastereoisomer Pd–allyl intermediates for **S1** with ligand **L1a**. The relative amounts of each isomer are shown in parentheses. The chemical shifts (in ppm) of the allylic terminal carbon atoms are also shown.

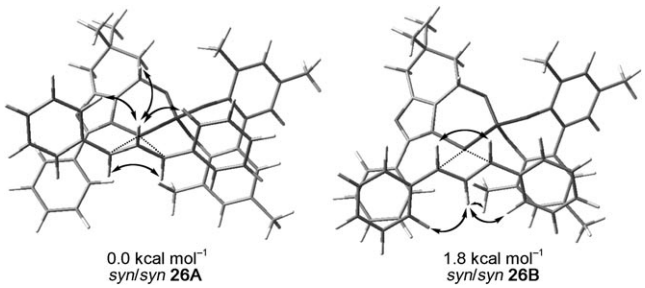

Figure 1. Calculated structures (DFT) for cationic species of complex [Pd(η^3-1,3-diphenylallyl)(**L1a**)]BF$_4$ (**26**) and their relative formation enthalpies. This figure also shows the relevant NOE contacts from the NOESY experiment.

The VT NMR spectroscopic study of Pd–allyl intermediate **27** containing ligand **L6a**, which forms a seven-membered chelate ring and provides lower enantioselectivity than Pd/**L1a**, also had a mixture of two *syn*/*syn endo* (**A**) and *exo* (**B**) isomers, but at a ratio of 1.25:1 (see the Experimental Section). Also, the more electrophilic allyl carbon terminus was *trans* to the phosphite moiety (Scheme 4). In contrast to the Pd/**L1a** catalytic system, the diastereoisomeric excess ($de = 11$ % (*S*)) of the Pd intermediates differed from the enantiomeric excess (21 % (*S*)) of alkylation product **15**. As shown by NMR spectroscopy,[20] isomer **A** reacts slightly faster than isomer **B**,[21] thus explaining this difference. However, the lower enantioselectivity with this system than with the previous Pd/**L1a** catalytic system can mainly be attributed to the decrease in the relative amount of isomer **A** with respect to isomer **B**, compared with the population of the isomers (**A** and **B**) for complex **26**.

Next, we studied the Pd–1,3-diphenylallyl intermediate **28** containing ligand **L4a**, which differs from **L1a** due to the presence of a bulky *tert*-butyl group at the oxazole moiety instead of a phenyl substituent and provides much lower enantioselectivity than the Pd/**L1a** catalyst. The VT NMR spectra indicated the presence of a mixture of two species at a ratio of 7:3 (see the Experimental Section). The major species were assigned by NOE to the *syn*/*syn endo* **A** isomer, whereas the minor species was attributed to com-

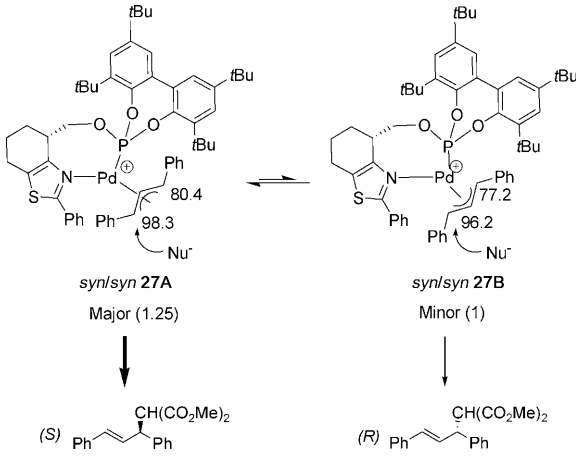

Scheme 4. Diastereoisomer Pd–allyl intermediates for **S1** with ligand **L6a**. The relative amounts of each isomer are shown in parentheses. The chemical shifts (in ppm) of the allylic terminal carbon atoms are also shown.

pound **C**, which contains two ligands coordinated in a monodentated fashion (Scheme 5).[22] The formation of **C** is due to the fact that the replacement of the phenyl ozaxole substituents in ligand **L1a** by a bulky *tert*-butyl group caused greater steric interaction with one of the phenyl substitutents of substrate **S1** in the related *syn*/*syn exo* **B** isomer observed in Pd/**L1a** complex **26** (Scheme 5). The formation of compound **C** minimizes this new steric interaction and explains why the expected *syn*/*syn exo* **B** isomer in solution was not detected (Scheme 5). Therefore, the fact that enantioselectivity was lower when the Pd/**L4a** catalyst was used (*ee* values up to 22%) than when the Pd/**L1a** catalyst was used (*ee* values up to 82%) may be due to the presence of Pd complex **C**. Complexes of this type are known to be faster and less enantioselective than their bidentate counterparts because they have more degrees of freedom.[11b,23]

Finally, we studied the cooperative effect observed between the configuration of the ligand backbone and the configuration of the biaryl phosphite moiety with complexes **29** and **30**, which contain ligands **L1d** and **L1e**, respectively. The VT NMR spectroscopic study indicated the presence of a mixture of two *syn*/*syn endo* (**A**) and *exo* (**B**) isomers in ratios of 5:1 and 1:2.5, respectively (Scheme 6). As for the 1,3-diphenylallyl intermediates discussed above, the NMR spectroscopic data showed that the more electrophilic allyl terminal carbon is *trans* to the phosphite moiety at the **A** isomers (**29A** and **30A**). For complex **29**, our results indicated that the stereochemical outcome of the re-

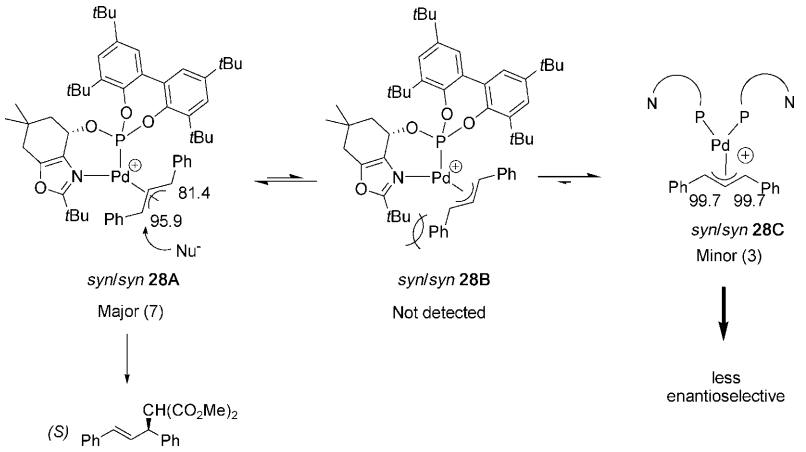

Scheme 5. Diastereoisomer Pd–allyl intermediates for **S1** with ligand **L4a**. The relative amounts of each isomer are shown in parentheses. The chemical shifts (in ppm) of the allylic terminal carbon atoms are also shown.

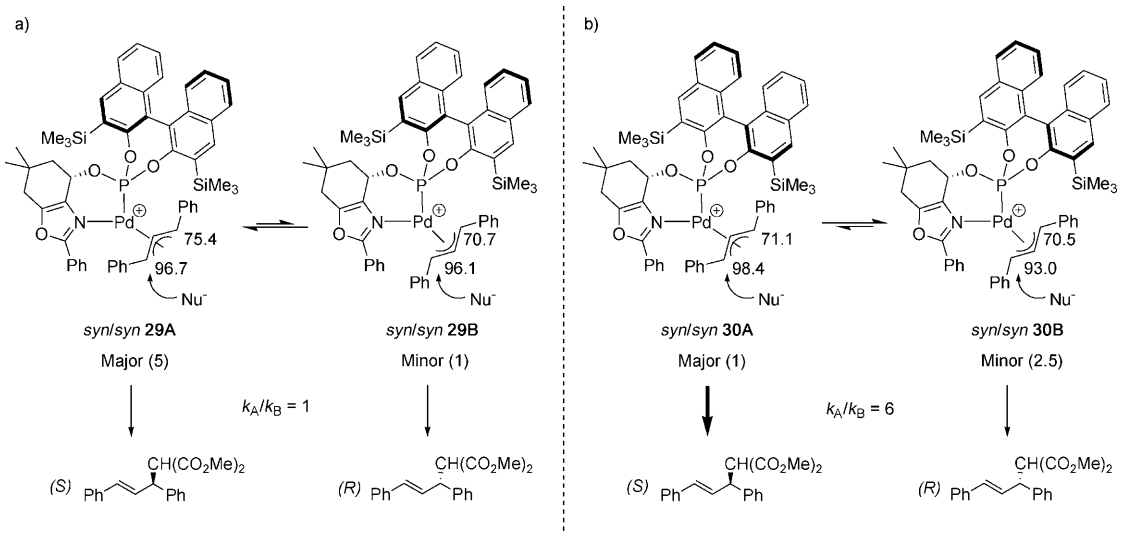

Scheme 6. Diastereoisomer Pd–allyl intermediates for **S1** with a) ligand **L1d** and b) ligand **L1e**. The relative amounts of each isomer are shown in parentheses. The chemical shifts (in ppm) of the allylic terminal carbon atoms are also shown.

action ($ee = 69\%$ (*S*)) was mainly due to the diastereoisomeric excess ($de = 66\%$ (*S*)) of the Pd complexes in solution, as observed for Pd/**L1a**. However, for complex **30**, the diastereoisomeric excess ($de = 43\%$ (*R*)) did not match the enantioselectivity obtained ($ee = 40\%$ (*S*)). Therefore, we conclude that isomer **30A** reacts faster than isomer **30B**. A clear indication of this fact can be found in the higher electrophilicity of the allylic terminal carbon *trans* to the phosphite in **30A** than in **30B** ($\Delta(\delta^{13}C) = 4.6$ ppm). Although isomer **30A** has a faster reaction rate than isomer **29A**, this is not the reason why Pd/**L1e** causes lower enantioselectivity than Pd/**L1d**. Rather, the lower enantioselectivity of Pd/**L1e** is because the relative amount of isomer **A** respect to isomer **B** is much lower in Pd/**L1e** than in Pd/**L1d.** Therefore, as observed earlier, the presence of an *S* configuration at the biaryl phosphite moiety is necessary for good enantioselectivity. In addition, these results provide further evidence that the flexible biphenyl phosphite moieties in ligands **L1a–c** adopt an *S* configuration when coordinated to palladium.

In summary, the study of the Pd–1,3-diphenylallyl intermediate showed that for enantioselectivity to be high, the different ligand parameters need to be correctly combined to predominantly form one of the Pd isomers and also to avoid the formation of species with ligands coordinated in a monodentated fashion.

Palladium–1,3-dimethylallyl complexes: When the phosphite–nitrogen ligand library **L1–L8a–g** was used in the allylic substitution of substrate **S3**, the catalytic results revealed a different trend with regard to the effect of the ligand parameters than with the hindered substrate **S1**. A seven-membered chelate ring, the presence of methyl substituents at the alkyl backbone chain, and a bulky (*S*)-binaphthyl phosphite moiety are necessary for high enantioselectivity. To understand this catalytic behavior, we studied Pd–π-allyl complexes **31–33**, which contain ligands **L1a**, **L7a**, and **L7e**, respectively. With ligands **L1a** and **L7a**, we studied the effect of the chelate ring size, whereas with ligand **L7e** we studied the configuration of the biaryl phosphite moiety.

The VT NMR (30 to −80 °C) spectroscopic study of Pd–allyl intermediate **31**, which contains ligand **L1a**, had a mixture of three isomers in equilibrium at a ratio of 2.5:1:2 (see the Experimental Section). Isomers **A** and **B** were assigned by NOE to the two *syn*/*syn endo* **A** and *exo* **B** isomers, whereas isomer **D** was assigned to the *syn*/*anti* isomer (Scheme 7). For isomers **A** and **B**, the NOE indicated interactions between the two terminal protons of the allyl group, whereas for isomer **D** the central allyl proton showed a NOE interaction with the terminal allyl proton located *trans* to the oxazole group (Figure 2). Moreover, for isomers **A** and **D**, the central allyl proton showed a NOE interaction with the hydrogen of the CH−O group of the ligand, whereas in isomer **B** this interaction appeared with the hydrogen atoms of the *tert*-butyl group. These interactions can be explained by assuming a *syn*/*syn endo* disposition for isomer **A**, a *syn*/*syn exo* disposition for isomer **B**, and a *syn*/*anti* disposition for isomer **D** (Figure 2). The NOESY also indicated an exchange between the allylic terminal protons located *trans* to the oxazole moiety of isomers **B** and **D** (Figure 2). This confirms the η^3–η^1–η^3 movement for the exchange between isomers **B** and **D**.[24] In addition, the fact that no other H_{anti}–H_{syn} exchange was observed indicates that the exchange took place by means of the selective opening of one of the terminal Pd−C bonds. The formation of isomer **D** is due to the fact that, in complex **B**, there was

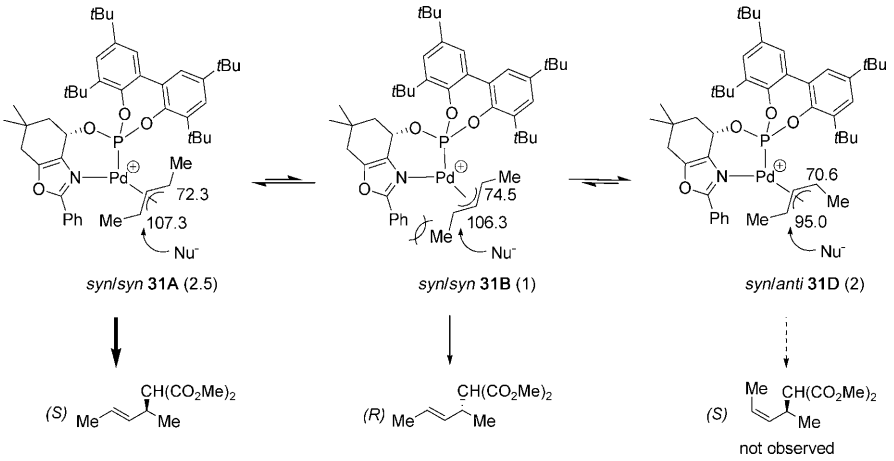

Scheme 7. Diastereoisomer Pd–allyl intermediates for **S3** with ligand **L1a**. The relative amounts of each isomer are shown in parentheses. The chemical shifts (in ppm) of the allylic terminal carbon atoms are also shown.

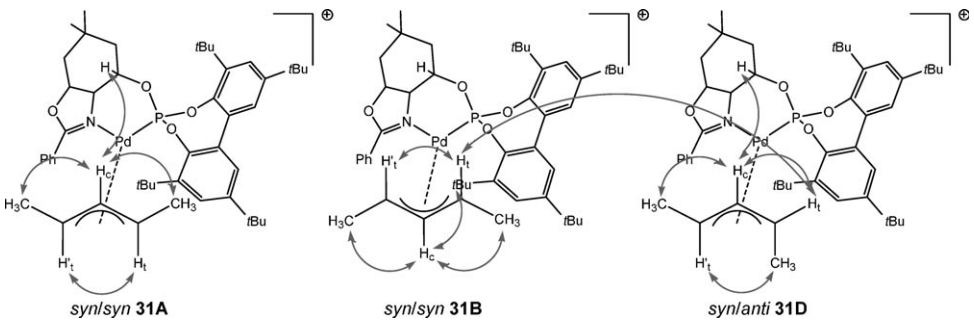

Figure 2. Relevant NOE contacts from the NOESY experiment of the [Pd(η^3-1,3-dimethylallyl)(**L1a**)]BF_4 (**31**) isomers.

an increase in the steric interaction between the oxazole phenyl group and one of the methyl substitutents of **S3** due to the absence of the favorable π-stacking interaction observed in the related Pd–1,3-diphenylallyl complex **26**. The formation of isomer **D** minimized this steric interaction (Scheme 7). Therefore, the open Pd–C bond belongs to the most electrophilic carbon atom containing the substituent that undergoes the biggest steric hindrance with the phenyl oxazole fragment. The NMR spectroscopic data also indicated that the most electrophilic allyl carbon terminus is *trans* to the phosphite moiety in *syn*/*syn* isomer **A** and in *syn*/*syn* isomer **B**, and that the allylic terminus carbon in isomer **D** is far less electrophilic ($\Delta(\delta^{13}C) > 11$ ppm). Assuming that the nucleophilic attack takes place at the most electrophilic allyl carbon terminus, on the basis of the observed stereochemical outcome of the reaction (59% *S* in product **18**), and since the *ee* of alkylation product **18** differs from the diastereoisomeric excess ($de = 41\%$ (*S*)) of the reacting Pd intermediates **A** and **B**, we conclude that isomer **A** reacts faster than isomer **B**. This was confirmed by an in situ NMR spectroscopic study of the reactivity of the Pd intermediates with sodium malonate at low temperature. This study indicated that isomer **31A** reacts approximately 1.5 times faster than isomer **31B**. This is also consistent with the fact that, for both isomers, the most electrophilic allylic terminal carbon atom is the one *trans* to the phosphite in the major **A** isomer.

The VT NMR spectroscopic study of Pd–allyl intermediate **32**, which contains ligand **L7a**, which forms a seven-membered chelate ring and provides higher enantioselectivity than Pd/**L1a**, also had a mixture of three isomers at a ratio of 5:1:7 (see the Experimental Section). Isomers **A**, **B**, and **D** were assigned by NOE to the *syn*/*syn endo*, *syn*/*syn exo*, and *syn*/*anti* isomers, respectively (see Scheme 8). Again, the most electrophilic allyl carbon terminus was *trans* to the phosphite moiety in *syn*/*syn* isomer **A** and *syn*/*syn* isomer **B**, and the allylic terminus carbon in isomer **D** was far less electrophilic ($\Delta(\delta^{13}C) > 11$ ppm). As observed for complex Pd/**L1a** (**31**), isomer **A** reacts faster than isomer **B**. The higher enantioselectivity with this system than with the Pd/**L1a** catalytic system discussed above can be attributed to the decrease in the relative amount of isomer **B** with respect to isomer **A** compared with the population of the isomers (**A** and **B**) for complex **31**. The decrease in the population of isomer **B** is due to the formation of a smaller chiral pocket with ligand **L7a** than with ligand **L1a**. This smaller chiral pocket creates a greater steric interaction between the thiazole phenyl group and one of the methyl substitutents of **S3**, which results in the preferential formation of the less electrophilic *syn*/*anti* isomer **D**.

Finally, the VT NMR spectroscopic study of Pd–allyl intermediate **33**, which contains ligand **L7d**, had a mixture of three isomers in a ratio of 10:1:9 (see the Experimental Section). Isomers **A**, **B**, and **D** were assigned by NOE to the *syn*/*syn endo*, *syn*/*syn exo*, and *syn*/*anti* isomers, respectively (Scheme 9). As for complexes **31** and **32**, the fastest-reacting isomer was the *syn*/*syn* isomer **A**, whereas isomer **D** was far less electrophilic and therefore did not play a direct role in

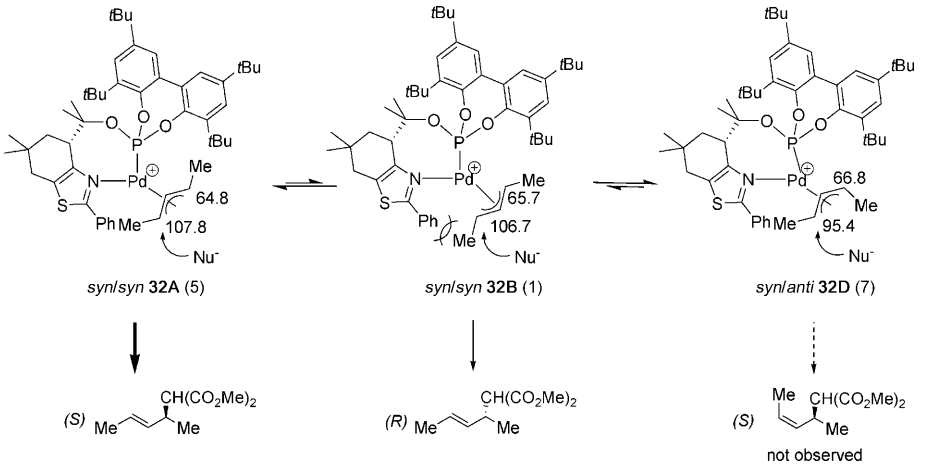

Scheme 8. Diastereoisomer Pd–allyl intermediates for **S3** with ligand **L7a**. The relative amounts of each isomer are shown in parentheses. The chemical shifts (in ppm) of the allylic terminal carbon atoms are also shown.

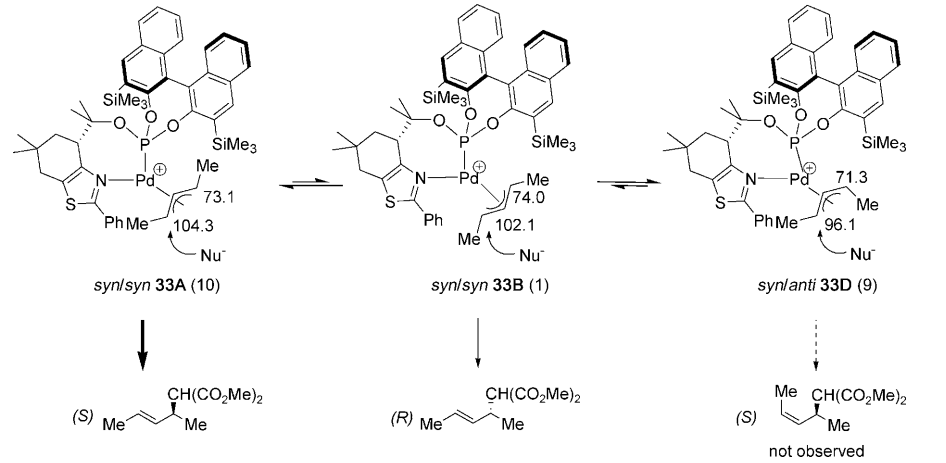

Scheme 9. Diastereoisomer Pd–allyl intermediates for **S3** with ligand **L7d**. The relative amounts of each isomer are shown in parentheses. The chemical shifts (in ppm) of the allylic terminal carbon atoms are shown.

the enantiodiscrimination process. The higher enantioselectivity obtained with Pd/**L7d** than with the Pd/**L7a** catalytic system is due to the larger amount of the most reactive isomer (isomer **A**) than in complex **32**.

In summary, for enantioselectivities to be high, the various ligand parameters need to be correctly combined to preferentially form the faster isomer **A**. The formation of this isomer is mainly governed by the size of the chelate ring and the configuration of the biaryl phosphite moiety.

Palladium–1,3-cyclohexenylallyl complexes: When the phosphite–nitrogen ligand library **L1**–**L8a**–**g** was used in the allylic substitution of cyclic substrates **S5** and **S6**, the catalytic results showed that the effect of the ligand parameters on enantioselectivity was different from the effect observed in the substitution of the linear substrates **S1** and **S2**. The best results were obtained with ligands **L1d** and **L1e**, which form a six-membered chelate ring, have phenyl substituents in the nitrogen heterocyclic ring, and have bulky enantiopure binaphthyl phosphite moieties. Interestingly, the sense of enantioselectivity was controlled by the configuration of the biaryl phosphite moiety. So, to understand this catalytic behavior, we studied Pd–π-allyl complexes **34** and **35**, which contain ligands **L1d** and **L1e**.

The VT NMR (35 to −80 °C) spectroscopic study of Pd intermediate **34**, which contains ligand **L1d**, showed a mixture of the two possible isomers at a ratio of 1:6, respectively (see Scheme 10). All isomers were unambiguously assigned by NOE to the isomers **A** and **B** (Figure 3). Thus, for isomer **A**, the NOE indicated interactions between the hydrogen of the CH−O group and the central allyl proton, whereas for isomer **B** this interaction appeared with one of the methylenic hydrogen atoms of the allyl ligand (Figure 3). The carbon NMR spectroscopic chemical shifts indicated that the most electrophilic allylic terminus carbon is *trans* to the phosphite moiety. The difference between the diastereoisomeric ratio and enantioselectivity observed in the alkylation of **S5** ($de = 70\,\%$ (*S*) vs. $ee = 80\,\%$ (*S*)) indicated that the nucleophile reacts faster with the major **B** isomer. This was confirmed by the reactivity of the Pd intermediate with sodium malonate at low temperature by in situ NMR spectroscopy.[25] We also carried out theoretical calculations at the DFT level. Figure 3 shows these calculated structures and their relative formation enthalpy values, with isomer **B** being the most stable. The difference in the calculated formation enthalpies of the two isomers ($\Delta H = 1.5$ Kcal mol^{-1}) is in agreement with the population observed by NMR spectroscopy.

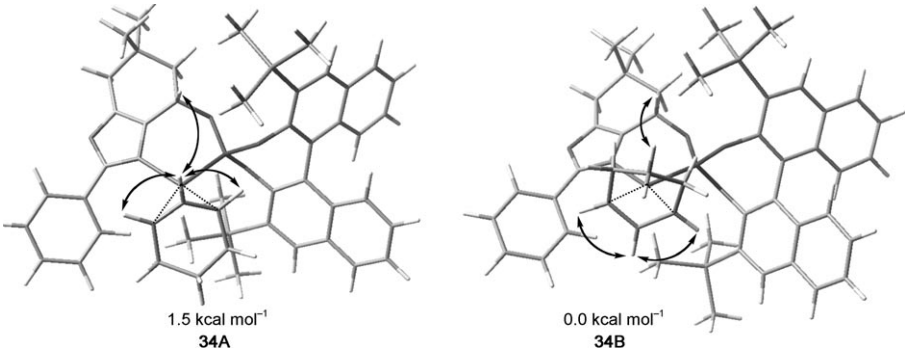

Figure 3. Calculated structures (DFT) for cationic species of complex [Pd(η^3-1,3-cyclohexenylallyl)(**L1a**)]BF_4 (**34**) and their relative formation enthalpies. This figure also shows the relevant NOE contacts from the NOESY experiment.

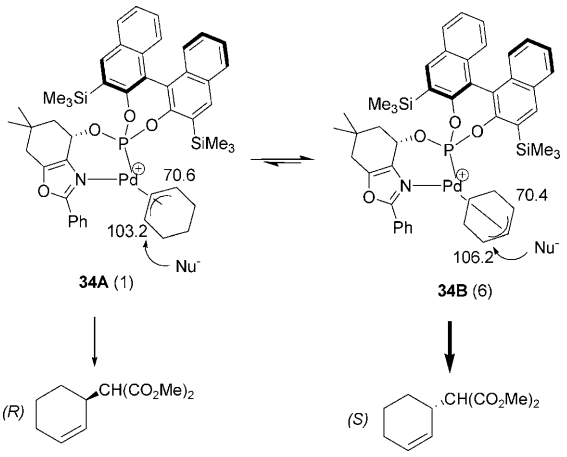

Scheme 10. Diastereoisomer Pd–allyl intermediates for **S5** with ligand **L1d**. The relative amounts of each isomer are shown in parentheses. The chemical shifts (in ppm) of the allylic terminal carbon atoms are also shown.

The VT NMR (35 °C to −80 °C) spectroscopic study of Pd intermediate **35**, which contains ligand **L1e**, also showed a mixture of the two possible isomers (**A** and **B**), but at a ratio of 6.5:1, respectively (Scheme 11). The carbon NMR spectroscopic chemical shifts also indicated that the most electrophilic allylic terminus carbon is *trans* to the phosphite moiety. In contrast to Pd intermediate **34**, the fastest-reacting isomer is **A**. This is in agreement with the fact that Pd/**L1e** provided a level of enantioselectivity similar to that of Pd/**L1d**, discussed above, but in the opposite enantiomer of the alkylation products **19** and **20**.

Conclusion

A new P,N-ligand library **L1**–**L8a**–**g** was synthesized for the Pd-catalyzed allylic substitution reactions of several substrates with different electronic and steric properties. These series of ligands have five main advantages: 1) they can be

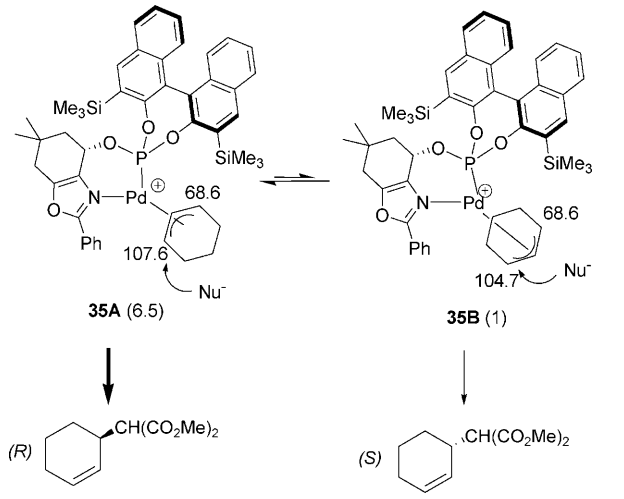

Scheme 11. Diastereoisomer Pd–allyl intermediates for **S5** with ligand **L1e**. The relative amounts of each isomer are shown in parentheses. The chemical shifts (in ppm) of the allylic terminal carbon atoms are also shown.

prepared efficiently from readily available hydroxyl–oxazole/thiazole derivatives; 2) the hydroxyl–oxazole/thiazole cores are much more robust than the usually used hydroxyl–oxazoline ones; 3) the flexibility and larger bite angle created by the biaryl phosphite moiety and the different bridge lengths increase versatility; 4) the π-acceptor character of the phosphite moiety increases reaction rates; and 5) their modular nature enables the bridge length, the substituents at the heterocyclic ring and in the alkyl backbone chain, the configuration of the ligand backbone, and the substituents/configurations in the biaryl phosphite moiety to be easily and systematically varied, so that activities and regio- and enantioselectivities can be maximized for each substrate as required. By carefully selecting the ligand components, therefore, high regio- and enantioselectivities (*ee* values up to 96%) and good activities were obtained in a broad range of mono-, di-, and trisubstituted linear hindered and unhindered substrates and cyclic substrates. Of particular note were the high regio- and enantioselectivities (up to 96% *ee*) combined with high activities obtained for the mono- and trisubstituted substrates **S7–S10**. In addition, for all substrates, both enantiomers of the substitution products were obtained with high enantioselectivities.

By studying the Pd–1,3-diphenylallyl, –1,3-dimethylallyl, and –1,3-cyclohexenylallyl intermediates by means of NMR spectroscopy and DFT calculations, we were able to better understand the observed catalytic behavior. For enantioselectivities to be high, we conclude that ligand parameters need to be correctly combined to predominantly form the Pd intermediate that has the fastest reaction with the nucleophile. We also found that the nucleophilic attack takes place predominantly at the allylic terminal carbon atom located *trans* to the phosphite moiety.

Experimental Section

General considerations: All reactions were carried out using standard Schlenk techniques under an atmosphere of argon. Solvents were purified and dried by standard procedures. Phosphorochloridites are easily prepared in one step from the corresponding biaryls.[26] Hydroxyl–oxazoles **6** and **7** and hydroxyl–thiazole **13** were prepared as previously described.[9] Racemic substrates **S1–S10** were prepared as previously reported.[27–30,14b] $[\{Pd(\eta^3\text{-}1,3\text{-}Ph_2\text{-}C_3H_3)(\mu\text{-}Cl)\}_2]$,[31] $[\{Pd(\eta^3\text{-}1,3\text{-}Me_2\text{-}C_3H_3)(\mu\text{-}Cl)\}_2]$,[32] and $[\{Pd(\eta^3\text{-cyclohexenyl})(\mu\text{-}Cl)\}_2]$[33] were prepared as previously described. ^1H, $^{13}C\{^1H\}$, and $^{31}P\{^1H\}$ NMR spectra were recorded using a 400 MHz spectrometer. Chemical shifts are relative to that of $SiMe_4$ (^1H and ^{13}C) as internal standard or H_3PO_4 (^{31}P) as external standard. ^1H, ^{13}C, and ^{31}P assignments were done based on ^1H,^1H gCOSY, ^1H,^{13}C gHSQC, and ^1H,^{31}P gHMBC experiments. Geometries of all substrates were optimized using the Jaguar program[34] by applying the B3LYP hybrid density functional[35] together with the LACVP** basis sets. Normal-mode analysis of stable structures revealed no imaginary frequencies, or a single imaginary frequency with negligibly low energy ($\tilde{\nu} < 100\ cm^{-1}$). LACVP in Jaguar defines a combination of the LANL2DZ basis set[36] for palladium and the 6-31G basis set for other atoms.

General procedure for the preparation of hydroxyl–oxazoles 8 and 9: Diazodimedone (2.00 g, 12 mmol) and the corresponding *para*-substituted benzonitrile (60 mmol for 4-methylbenzonitrile and 14 mmol for 4-(trifluoromethyl)benzonitrile) were heated in an oil bath at 60°C and $Rh(OAc)_2$ (10 mg, 0.045 mmol) was added. The reaction was stirred for 1.5 h, and if starting material remained, another portion of $Rh(OAc)_2$ (10 mg, 0.045 mmol) was added. After an additional 1.5 h, the reaction was cooled to room temperature and purified by chromatography on silica (pentane/ethyl acetate 75:25 to 25:75) to give the ketone–oxazoles as white solids. Compound **3** (2.02 g, 66% yield): ^1H NMR ($CDCl_3$): δ = 1.21 (s, 6H; 2×CH_3), 2.41 (s, 3H; CH_3), 2.50 (s, 2H; CH_2), 2.90 (s, 2H; CH_2), 7.24–7.29 (m, 2H; Ar), 7.97–8.02 ppm (m, 2H; Ar). Compound **4** (1.53 g, 51% yield): ^1H NMR ($CDCl_3$): δ = 1.22 (s, 6H; 2×CH_3), 2.52 (s, 2H; CH_2), 2.93 (s, 2H; CH_2), 7.71–7.75 (m, 2H; Ar), 8.20–8.25 ppm (m, 2H; Ar).

For the reduction of the ketone–oxazoles, $BH_3{\cdot}SMe_2$ (2.1 equiv) and (*R*)-Me-CBS (0.1 equiv) were dissolved in THF (5 mL for 4 mmol $BH_3{\cdot}SMe_2$) at 0°C and stirred for 1 h. The temperature was raised to ambient and a solution of ketone (1 equiv) in THF/toluene (4:1 mL for 2 mmol ketone) was added over 2 h using a syringe pump. The reaction was stirred for an additional hour, cooled to 0°C, and quenched with methanol. The solvent was evaporated and the resulting oil was purified by chromatography on silica (pentane/ethyl acetate 25:75) to afford hydroxyl–oxazoles **8** and **9** as white solids (72% *ee* for **8** and 78% *ee* for **9**). The enantiomeric excess could not be increased by recrystallization. The enantiomers were separated by chiral chromatography on semipreparative HPLC using a 250×20 mm Chiralcel OD column (hexane/isopropanol 95:5, 5 mL min^{-1}) to give *ee* > 99%. Hydroxyl–oxazole **8**: ^1H NMR ($CDCl_3$): δ = 1.03 (s, 3H; CH_3), 1.19 (s, 3H; CH_3), 1.67 (dd, *J* = 13.2, 8.0 Hz, 1H; CH_2), 1.99 (ddd, *J* = 13.4, 6.0, 1.5 Hz, 1H; CH_2), 2.38 (s, 3H; CH_3–Ph), 2.45 (m, 1H; CH_2), 2.59 (dd, *J* = 16.4, 2.2 Hz, 1H; CH_2), 3.66 (brs, 1H; OH), 4.85 (m, 1H; CH), 7.18–7.28 (m, 2H; CH=), 7.87–7.95 ppm (m, 2H; CH=); ^{13}C NMR ($CDCl_3$): δ = 24.5, 26.9, 30.6, 33.0, 35.6, 45.5, 62.9, 124.9, 126.1, 129.4, 136.0, 140.3, 147.3, 161.3 ppm; elemental analysis calcd (%) for $C_{16}H_{19}NO_2$: C 74.68, H 7.44, N 5.44; found: C 74.47, H 7.50, N 5.43. Hydroxyl–oxazole **9**: ^1H NMR ($CDCl_3$): δ = 1.05 (s, 3H; CH_3), 1.21 (s, 3H; CH_3), 1.68 (dd, *J* = 13.3, 8.1 Hz, 1H; CH_2), 2.02 (dd, *J* = 13.3, 6.0 Hz, 1H; CH_2), 2.50 (d, *J* = 16.8 Hz, 1H; CH_2), 2.63 (d, *J* = 16.8 Hz, 1H; CH_2), 3.27 (brs, 1H; OH), 4.87 (m, 1H; CH), 7.63–7.74 (m, 2H; CH=), 8.07–8.18 ppm (m, 2H; CH=); ^{13}C NMR ($CDCl_3$): δ = 27.2, 30.8, 33.3, 35.9, 45.7, 63.2, 126.0, 126.1, 126.6, 131.0, 137.0, 149.0, 160.0 ppm; elemental analysis calcd (%) for $C_{16}H_{16}F_3NO_2$: C 61.73, H 5.18, N 4.50; found: C 61.79, H 5.23, N 4.52.

Preparation of hydroxyl–oxazole 10: Diazodimedone (5.00 g, 30.1 mmol), pivalonitrile (12.5 g, 150 mmol), and $Rh(OAc)_2$ (27 mg, 0.12 mmol) were heated in an oil bath at 60°C. The reaction was stirred for 1 h, cooled to room temperature, and purified by chromatography on silica (pentane/

ethyl acetate 75:25 to 25:75) to give ketone–oxazole **5** as a white solid (4.23 g, 68% yield). ^{1}H NMR ($CDCl_3$): δ = 1.16 (s, 6H; 2×CH_3), 1.39 (s, 9H; 3×CH_3), 2.41 (s, 2H; CH_2), 2.78 ppm (s, 2H; CH_2).

For the reduction of the ketone–oxazole, ketone (2.22 g, 10 mmol) was dissolved in 95% ethanol (125 mL), and $NaBH_4$ (1.14 g, 30 mmol) was added. The reaction was stirred and followed by TLC. The reaction was quenched with 1 M HCl and extracted with dichloromethane (2×25 mL). The organic phase was dried over $MgSO_4$, filtered, and concentrated to give racemic hydroxyl–oxazole **10** as a white solid (1.94 g, 87% yield). The enantiomers were separated by chiral chromatography on semipreparative HPLC using a (250×20 mm) Chiralcel OD column (hexane/isopropanol 98:2, 5 mL min^{-1}) to give *ee* > 99%. ^{1}H NMR ($CDCl_3$): δ = 0.96 (s, 3H; CH_3), 1.11 (s, 3H; CH_3), 1.32 (s, 9H; CH_3, *t*Bu), 1.57 (dd, *J* = 3.2, 8.0 Hz, 1H; CH_2), 1.86 (ddd, *J* = 13.2, 5.9, 1.4 Hz, 1H; CH_2), 2.30 (dt, *J* = 16.2, 1.6 Hz, 1H; CH_2), 2.45 (dd, *J* = 16.2, 2.1 Hz, 1H; CH_2), 4.52 (br s, 1H; OH), 4.74 ppm (m, 1H; CH); ^{13}C NMR ($CDCl_3$): δ = 26.8, 28.5, 30.5, 30.6, 32.9, 33.7, 35.4, 45.5, 62.0, 62.2, 134.2, 146.4, 170.4 ppm; elemental analysis calcd (%) for $C_{13}H_{21}NO_2$: C 69.92, H 9.48, N 6.27; found: C 69.89, H 9.52, N 6.22.

Preparation of hydroxyl–thiazole 14: $CeCl_3$·7H_2O (3.15 g) was dried in a vacuum oven at 120°C overnight. A flask with dry $CeCl_3$ (2.00 g, 8.10 mmol) was cooled under nitrogen in an ice bath, THF was added (30 mL), and the suspension was stirred at room temperature overnight. After cooling in an ice bath, a 3 M solution of MeMgCl (4 mL, 12.0 mmol) was added. Suspension was stirred for 2 h and a solution of thiazole ester[9b] (0.65 g, 2.26 mmol) was added in THF (10 mL). After stirring overnight, the reaction was cooled in an ice bath and quenched by addition of saturated NH_4Cl solution (50 mL), and stirred for 1 h. Water (50 mL) was added, THF was evaporated, and the product was extracted with diethyl ether (2 times). After drying the organic phase over $MgSO_4$, filtering, and evaporation of the solvent, crude material was purified by chromatography on silica (pentane/ethyl acetate 100:0 to 95:5) to give hydroxyl–thiazole **14** as a white solid (0.44 g, 71% yield). The resolution of enantiomers was achieved on semipreparative HPLC using a (250×20 mm) Chiralcel OD column (hexane/isopropanol 95:5, 5 mL min^{-1}) to give both enantiomers with *ee* > 99%. ^{1}H NMR ($CDCl_3$): δ = 1.01 (s, 3H; CH_3), 1.32 (s, 3H; CH_3), 1.39 (m, 1H; CH_2), 1.74 (m, 1H; CH_2), 2.02–2.15 (m, 2H; CH_2), 2.73 (m, 1H; CH_2), 2.85 (m, 1H; CH_2), 2.99 (m, 1H; CH_2), 6.48 (br s, 1H; OH), 7.33–7.46 (m, 2H; CH=), 7.80–7.92 ppm (m, 2H; CH=); ^{13}C NMR ($CDCl_3$): δ = 23.1, 23.8, 24.2, 26.2, 27.7, 48.4, 73.5, 126.1, 128.8, 129.8, 131.1, 133.1, 152.4, 164.2 ppm; elemental analysis calcd (%) for $C_{16}H_{19}NOS$: C 70.29, H 7.00, N 5.12; found: C 70.35, H 7.02, N 5.11.

General procedure for the preparation of phosphite–nitrogen ligands L1–L8a–g: Phosphorochloridite (2.2 mmol) produced in situ was dissolved in toluene (5 mL) and pyridine (0.36 mL, 4.6 mmol) was added. Hydroxyl–oxazole or hydroxyl–thiazole (2 mmol) was azeotropically dried with toluene (3×1 mL) and then dissolved in toluene (10 mL), to which pyridine (0.36 mL, 4.6 mmol) was added. The alcohol solution was transferred slowly at 0°C to the solution of phosphorochloridite. The reaction mixture was warmed up to 80°C and stirred overnight, and the pyridine salts were removed by filtration. Evaporation of the solvent gave a white foam, which was purified by flash chromatography (toluene/hexane/NEt_3) to produce the corresponding ligand as a white powder.

Ligand L1a: Yield: 826 mg (60%); ^{31}P NMR (C_6D_6): δ = 148.7 ppm; ^{1}H NMR (C_6D_6): δ = 0.57 (s, 3H; CH_3), 0.77 (s, 3H; CH_3), 1.23 (s, 9H; CH_3, *t*Bu), 1.25 (s, 9H; CH_3, *t*Bu), 1.57 (m, 1H; CH_2), 1.61 (s, 9H; CH_3, *t*Bu), 1.69 (s, 9H; CH_3, *t*Bu), 1.73 (m, 1H; CH_2), 1.92 (m, 1H; CH_2–C=), 2.08 (m, 1H; CH_2–C=), 5.53 (m, 1H; CH–O), 7.1–8.2 ppm (m, 9H; CH=); ^{13}C NMR (C_6D_6): δ = 27.7 (CH_3), 29.9 (CH_3), 31.9 (CH_3, *t*Bu), 33.1 (C, *t*Bu), 35.0 (CH_2–C=), 36.2 (CMe_2), 45.1 (CH_2), 67.8 (d, *J*(C,P) = 12.2 Hz; CH–O), 124–165 ppm (aromatic carbon atoms); elemental analysis calcd (%) for $C_{43}H_{56}NO_4P$: C 75.74, H 8.28, N 2.05; found: C 75.82, H 8.11, N 2.11.

Ligand L1b: Yield: 725 mg (58%); ^{31}P NMR (C_6D_6): δ = 148.6 ppm; ^{1}H NMR (C_6D_6): δ = 0.60 (s, 3H; CH_3), 0.82 (s, 3H; CH_3), 1.55 (s, 9H; CH_3, *t*Bu), 1.62 (s, 9H; CH_3, *t*Bu), 1.77 (m, 1H; CH_2), 1.80 (m, 1H; CH_2), 1.97 (m, 1H; CH_2–C=), 2.12 (m, 1H; CH_2–C=), 3.28 (s, 3H; CH_3–O), 3.29 (s, 3H; CH_3–O), 5.52 (m, 1H; CH–O), 6.7–8.2 ppm (m, 9H; CH=); ^{13}C NMR (C_6D_6): δ = 27.8 (CH_3), 29.2 (CH_3), 30.0 (CMe_2), 31.6 (CH_3, *t*Bu), 31.8 (CH_3, *t*Bu), 33.0 (C, *t*Bu), 35.6 (CH_2–C=), 45.1 (CH_2), 55.4 (CH_3–O), 55.5 (CH_3–O), 67.9 (d, *J*(C,P) = 13 Hz; CH–O), 126–156 ppm (aromatic carbon atoms); elemental analysis calcd (%) for $C_{37}H_{44}NO_6P$: C 70.57, H 7.04, N 2.22; found: C 70.52, H 7.09, N 2.31.

Ligand L1c: Yield: 722 mg (59%); ^{31}P NMR (C_6D_6): δ = 147.8 ppm; ^{1}H NMR (C_6D_6): δ = 0.44 (s, 9H; CH_3–Si), 0.55 (s, 9H; CH_3–Si), 0.59 (s, 3H; CH_3), 0.81 (s, 3H; CH_3), 1.58 (m, 1H; CH_2), 1.76 (m, 1H; CH_2), 1.96 (m, 1H; CH_2–C=), 2.13 (m, 1H; CH_2–C=), 5.50 (m, 1H; CH–O), 6.9–8.3 ppm (m, 11H; CH=); ^{13}C NMR (C_6D_6): δ = 0.8 (CH_3–Si), 0.9 (CH_3–Si), 27.9 (CH_3), 30.2 (CH_3), 33.2 (CMe_2), 35.9 (CH_2–C=), 45.3 (CH_2), 67.8 (d, *J*(C,P) = 8.4 Hz; CH–O), 123–150 ppm (aromatic carbon atoms); elemental analysis calcd (%) for $C_{33}H_{40}NO_4PSi_2$: C 65.86, H 6.70, N 2.33; found: C 65.92, H 6.72, N 2.31.

Ligand L1d: Yield: 698 mg (49%); ^{31}P NMR (C_6D_6): δ = 146.3 ppm; ^{1}H NMR (C_6D_6): δ = 0.45 (s, 3H; CH_3), 0.54 (s, 9H; CH_3–Si), 0.73 (s, 9H; CH_3–Si), 0.82 (s, 3H; CH_3), 1.57 (m, 1H; CH_2), 1.88 (m, 1H; CH_2), 2.11 (m, 2H; CH_2–C=), 5.02 (m, 1H; CH–O), 6.9–8.3 ppm (m, 15H; CH=); ^{13}C NMR (C_6D_6): δ = 0.5 (CH_3–Si), 1.0 (CH_3–Si), 27.9 (CH_3), 29.7 (CH_3), 32.8 (CMe_2), 35.6 (CH_2–C=), 45.5 (CH_2), 70.2 (CH–O), 123–161 ppm (aromatic carbon atoms); elemental analysis calcd (%) for $C_{41}H_{44}NO_4PSi_2$: C 70.15, H 6.32, N 2.00; found: C 70.22, H 6.35, N 2.01.

Ligand L1e: Yield: 536 mg (39%); ^{31}P NMR (C_6D_6): δ = 147.4 ppm; ^{1}H NMR (C_6D_6): δ = 0.33 (s, 3H; CH_3), 0.55 (s, 9H; CH_3–Si), 0.65 (s, 3H; CH_3), 0.68 (s, 9H; CH_3–Si), 1.34 (m, 1H; CH_2), 1.61 (m, 1H; CH_2), 1.89 (m, 1H; CH_2–C=), 2.06 (m, 1H; CH_2–C=), 5.49 (m, 1H; CH–O), 6.9–8.3 ppm (m, 15H; CH=); ^{13}C NMR (C_6D_6): δ = 0.3 (CH_3–Si), 0.4 (CH_3–Si), 26.5 (CH_3), 29.6 (CH_3), 32.4 (CMe_2), 35.1 (CH_2–C=), 44.3 (CH_2), 66.8 (d, *J*(C,P) = 7.2 Hz; CH–O), 123–160 ppm (aromatic carbon atoms); elemental analysis calcd (%) for $C_{41}H_{44}NO_4PSi_2$: C 70.15, H 6.32, N 2.00; found: C 70.19, H 6.29, N 1.97.

Ligand L1f: Yield: 712 mg (64%); ^{31}P NMR (C_6D_6): δ = 138.7 ppm; ^{1}H NMR (C_6D_6): δ = 0.42 (s, 3H; CH_3), 0.78 (s, 3H; CH_3), 1.48 (dd, ^2J(H,H) = 14 Hz, ^3J(H,H) = 5.6 Hz, 1H; CH_2), 1.71 (dd, ^2J(H,H) = 14 Hz, ^3J(H,H) = 5.6 Hz, 1H; CH_2), 1.84 (m, ^2J(H,H) = 16 Hz, 1H; CH_2–C=), 2.06 (d, ^2J(H,H) = 16 Hz, 1H; CH_2–C=), 5.34 (m, 1H; CH–O), 6.9–8.3 ppm (m, 17H; CH=); ^{13}C NMR (C_6D_6): δ = 28.0 (CH_3), 29.4 (CH_3), 32.7 (CH_2–C=), 35.7 (CMe_2), 45.2 (CH_2), 68.5 (d, *J*(C,P) = 4.7 Hz; CH–O), 122–162 ppm (aromatic carbon atoms); elemental analysis calcd (%) for $C_{35}H_{28}NO_4P$: C 75.39, H 5.06, N 2.51; found: C 75.42, H 5.11, N 2.50.

Ligand L1g: Yield: 849 mg (76%); ^{31}P NMR (C_6D_6): δ = 153.1 ppm; ^{1}H NMR (C_6D_6): δ = 0.51 (s, 3H; CH_3), 0.72 (s, 3H; CH_3), 1.50 (dd, ^2J(H,H) = 12.4 Hz, ^3J(H,H) = 5.6 Hz, 1H; CH_2), 1.59 (dd, ^2J(H,H) = 12.4 Hz, ^3J(H,H) = 7.2 Hz, 1H; CH_2), 1.92 (m, ^2J(H,H) = 16.4 Hz, 1H; CH_2–C=), 2.01 (d, ^2J(H,H) = 16.4 Hz, 1H; CH_2–C=), 5.43 (m, 1H; CH–O), 6.8–8.3 ppm (m, 17H; CH=); ^{13}C NMR (C_6D_6): δ = 28.1 (CH_3), 29.7 (CH_3), 32.8 (CH_2–C=), 35.6 (CMe_2), 45.0 (d, *J*(C,P) = 3.1 Hz; CH_2), 67.8 (d, *J*(C,P) = 20.1 Hz; CH–O), 122–162 ppm (aromatic carbon atoms); elemental analysis calcd (%) for $C_{35}H_{28}NO_4P$: C 75.39, H 5.06, N 2.51; found: C 75.35, H 5.13, N 2.48.

Ligand L2a: Yield: 587 mg (42%); ^{31}P NMR (C_6D_6): δ = 148.0 ppm; ^{1}H NMR (C_6D_6): δ = 0.78 (s, 3H; CH_3), 0.98 (s, 3H; CH_3), 1.44 (s, 9H; CH_3, *t*Bu), 1.46 (s, 9H; CH_3, *t*Bu), 1.79 (m, 1H; CH_2), 1.83 (s, 9H; CH_3, *t*Bu), 1.91 (s, 9H; CH_3, *t*Bu), 1.95 (m, 1H; CH_2), 2.19 (m, 2H; CH_2–C=), 2.28 (m, 3H; CH_3–Ph), 5.75 (m, 1H; CH–O), 7.1–8.4 ppm (m, 8H; CH=); ^{13}C NMR (C_6D_6): δ = 21.7 (CH_3–Ph), 27.8 (CH_3), 30.0 (CH_3), 31.9 (CH_3, *t*Bu), 32.0 (CH_3, *t*Bu), 33.1 (C, *t*Bu), 36.2 (CH_2–C=), 36.7 (CMe_2), 45.1 (CH_2), 67.9 (d, *J*(C,P) = 17 Hz; CH–O), 124–164 ppm (aromatic carbon atoms); elemental analysis calcd (%) for $C_{44}H_{58}NO_4P$: C 75.94, H 8.40, N 2.01; found: C 75.89, H 8.41, N 2.0.5.

Ligand L2d: Yield: 698 mg (49%); ^{31}P NMR (C_6D_6): δ = 146.3 ppm; ^{1}H NMR (C_6D_6): δ = 0.43 (s, 3H; CH_3), 0.51 (s, 9H; CH_3–Si), 0.70 (s, 9H; CH_3–Si), 0.80 (s, 3H; CH_3), 1.52 (m, 1H; CH_2), 1.72 (m, 1H; CH_2), 2.18 (m, 2H; CH_2–C=), 2.23 (m, 3H; CH_3–Ph), 5.11 (m, 1H; CH–O), 6.9–8.3 ppm (m, 15H; CH=); ^{13}C NMR (C_6D_6): δ = 0.4 (CH_3–Si), 0.6 (CH_3–Si), 20.9 (CH_3–Ph), 27.8 (CH_3), 29.2 (CH_3), 33.8 (CMe_2), 35.8 (CH_2–C=), 45.6 (CH_2), 69.8 (CH–O), 123–161 ppm (aromatic carbon atoms); ele-

mental analysis calcd (%) for $C_{42}H_{46}NO_4PSi_2$: C 70.46, H 6.48, N 1.96; found: C 70.52, H 6.49, N 2.00.

Ligand L2e: Yield: 623 mg (44%); ^{31}P NMR (C_6D_6): δ = 146.9 ppm; ^{1}H NMR (C_6D_6): δ = 0.49 (s, 3H; CH_3), 0.510 (s, 9H; CH_3–Si), 0.66 (s, 9H; CH_3–Si), 0.76 (s, 3H; CH_3), 1.69 (m, 2H; CH_2), 2.21 (m, 2H; CH_2–C=), 2.25 (m, 3H; CH_3–Ph), 5.16 (m, 1H; CH–O), 6.9–8.3 ppm (m, 15H; CH=); ^{13}C NMR (C_6D_6): δ = −0.2 (CH_3–Si), 0.1 (CH_3–Si), 21.1 (CH_3–Ph), 27.9 (CH_3), 29.5 (CH_3), 33.9 (CMe_2), 36.2 (CH_2–C=), 45.3 (CH_2), 70.1 (CH–O), 123–161 ppm (aromatic carbon atoms); elemental analysis calcd (%) for $C_{42}H_{46}NO_4PSi_2$: C 70.46, H 6.48, N 1.96; found: C 70.49, H 6.51, N 1.99.

Ligand L3a: Yield: 674 mg (45%); ^{31}P NMR (C_6D_6): δ = 147.8 ppm; ^{1}H NMR (C_6D_6): δ = 0.61 (s, 3H; CH_3), 0.81 (s, 3H; CH_3), 1.28 (s, 9H; CH_3, *t*Bu), 1.29 (s, 9H; CH_3, *t*Bu), 1.60 (m, 1H; CH_2), 1.65 (s, 9H; CH_3, *t*Bu), 1.74 (s, 9H; CH_3, *t*Bu), 1.77 (m, 1H; CH_2), 1.97 (m, 1H; CH_2–C=), 2.12 (m, 1H; CH_2–C=), 5.55 (m, 1H; CH–O), 7.0–8.1 ppm (m, 8H; CH=); ^{13}C NMR (C_6D_6): δ = 27.6 (CH_3), 30.0 (CH_3), 31.9 (CH_3, *t*Bu), 32.0 (CH_3, *t*Bu), 33.1 (CMe_2), 35.0 (C, *t*Bu), 35.7 (C, *t*Bu), 36.2 (CH_2–C=), 45.0 (CH_2), 67.5 (d, *J*(C,P) = 11.5 Hz; CH–O), 124–160 ppm (aromatic carbon atoms); elemental analysis calcd (%) for $C_{44}H_{55}F_3NO_4P$: C 70.47, H 7.39, N 1.87; found: C 70.57, H 7.42, N 1.89.

Ligand L3c: Yield: 593 mg (44%); ^{31}P NMR (C_6D_6): δ = 146.8 ppm; ^{1}H NMR (C_6D_6): δ = 0.39 (s, 9H; CH_3–Si), 0.49 (s, 9H; CH_3–Si), 0.53 (s, 3H; CH_3), 0.77 (s, 3H; CH_3), 1.52 (m, 1H; CH_2), 1.69 (m, 1H; CH_2), 1.95 (m, 1H; CH_2–C=), 2.12 (m, 1H; CH_2–C=), 5.42 (m, 1H; CH–O), 6.9–8.1 ppm (m, 10H; CH=); ^{13}C NMR (C_6D_6): δ = 0.9 (CH_3–Si), 1.0 (CH_3–Si), 27.7 (CH_3), 30.3 (CH_3), 33.2 (CMe_2), 35.9 (CH_2–C=), 45.0 (CH_2), 67.5 (d, *J*(C,P) = 6.1 Hz; CH–O), 124–160 ppm (aromatic carbon atoms); elemental analysis calcd (%) for $C_{34}H_{39}F_3NO_4PSi_2$: C 60.97, H 5.87, N 2.09; found: C 60.99, H 5.89, N 2.07.

Ligand L3e: Yield: 676 mg (43%); ^{31}P NMR (C_6D_6): δ = 146.3 ppm; ^{1}H NMR (C_6D_6): δ = 0.43 (s, 3H; CH_3), 0.51 (s, 9H; CH_3–Si), 0.62 (s, 3H; CH_3), 0.65 (s, 9H; CH_3–Si), 1.34 (m, 1H; CH_2), 1.56 (m, 1H; CH_2), 1.84 (m, 1H; CH_2–C=), 2.02 (m, 1H; CH_2–C=), 5.42 (m, 1H; CH–O), 6.8–8.1 ppm (m, 14H; CH=); ^{13}C NMR (C_6D_6): δ = 1.0 (CH_3–Si), 1.1 (CH_3–Si), 27.0 (CH_3), 30.3 (CH_3), 33.2 (CMe_2), 35.8 (CH_2–C=), 45.0 (CH_2), 67.2 (d, *J*(C,P) = 5.3 Hz; CH–O), 123–160 ppm (aromatic carbon atoms); elemental analysis calcd (%) for $C_{42}H_{43}F_3NO_4PSi_2$: C 65.52, H 5.63, N 1.82; found: C 65.34, H 5.59, N 1.86.

Ligand L4a: Yield: 652 mg (49%); ^{31}P NMR (C_6D_6): δ = 148.0 ppm; ^{1}H NMR (C_6D_6): δ = 0.59 (s, 3H; CH_3), 0.80 (s, 3H; CH_3), 1.28 (s, 9H; CH_3, *t*Bu), 1.29 (s, 9H; CH_3, *t*Bu), 1.40 (s, 9H; CH_3, *t*Bu), 1.56 (m, 1H; CH_2), 1.66 (s, 9H; CH_3, *t*Bu), 1.71 (s, 9H; CH_3, *t*Bu), 1.75 (m, 1H; CH_2), 1.98 (m, 1H; CH_2–C=), 2.14 (m, 1H; CH_2–C=), 5.52 (m, 1H; CH–O), 7.0–7.7 ppm (m, 4H; CH=); ^{13}C NMR (C_6D_6): δ = 27.8 (CH_3), 29.2 (CH_3), 29.9 (CH_3, *t*Bu), 32.0 (CH_3, *t*Bu), 32.2 (CH_3, *t*Bu), 33.1 (CMe_2), 34.4 (C, *t*Bu), 35.0 (C, *t*Bu), 36.1 (CH_2–C=), 36.2 (C, *t*Bu), 45.3 (CH_2), 68.1 (d, *J*(C,P) = 12 Hz; CH–O), 124–170 ppm (aromatic carbon atoms); elemental analysis calcd (%) for $C_{41}H_{60}NO_4P$: C 74.40, H 9.14, N 2.12; found: C 74.45, H 9.18, N 2.08.

Ligand L4c: Yield: 709 mg (61%); ^{31}P NMR (C_6D_6): δ = 148.2 ppm; ^{1}H NMR (C_6D_6): δ = 0.49 (s, 9H; CH_3–Si), 0.54 (s, 9H; CH_3–Si), 0.57 (s, 3H; CH_3), 0.78 (s, 3H; CH_3), 1.21 (s, 9H; CH_3, *t*Bu), 1.45 (m, 1H; CH_2), 1.69 (m, 1H; CH_2), 1.96 (m, 1H; CH_2–C=), 2.19 (m, 1H; CH_2–C=), 5.48 (m, 1H; CH–O), 6.9–7.8 (m, 6H; CH=); ^{13}C NMR (C_6D_6): δ = 0.2 (CH_3–Si), 0.4 (CH_3–Si), 27.9 (CH_3), 29.8 (CH_3), 30.2 (CH_3, *t*Bu), 33.2 (CMe_2), 36.3 (CH_2–C=), 45.5 (CH_2), 68.3 (d, *J*(C,P) = 10 Hz; CH–O), 123–155 ppm (aromatic carbon atoms); elemental analysis calcd (%) for $C_{31}H_{44}NO_4PSi_2$: C 63.99, H 7.62, N 2.41; found: C 64.03, H 7.65, N 2.39.

Ligand L5a: Yield: 843 mg (62%); ^{31}P NMR (C_6D_6): δ = 148.7 ppm; ^{1}H NMR (C_6D_6): δ = 0.57 (s, 3H; CH_3), 0.77 (s, 3H; CH_3), 1.23 (s, 9H; CH_3, *t*Bu), 1.25 (s, 9H; CH_3, *t*Bu), 1.57 (m, 1H; CH_2), 1.61 (s, 9H; CH_3, *t*Bu), 1.69 (s, 9H; CH_3, *t*Bu), 1.73 (m, 1H; CH_2), 1.92 (m, 1H; CH_2–C=), 2.08 (m, 1H; CH_2–C=), 5.53 (m, 1H; CH–O), 7.1–8.2 ppm (m, 9H; CH=); ^{13}C NMR (C_6D_6): δ = 27.7 (CH_3), 29.9 (CH_3), 31.9 (CH_3, *t*Bu), 33.1 (C, *t*Bu), 35.0 (CH_2–C=), 36.2 (CMe_2), 45.1 (CH_2), 67.8 (d, *J*(C,P) = 12.2 Hz; CH–O), 124–165 ppm (aromatic carbon atoms); elemental analysis calcd (%) for $C_{43}H_{56}NO_4P$: C 75.74, H 8.28, N 2.05; found: C 75.72, H 8.31, N 2.01.

Ligand L6a: Yield: 738 mg (54%); ^{31}P NMR (C_6D_6): δ = 137.9 ppm; ^{1}H NMR (C_6D_6): δ = 1.43 (s, 9H; CH_3, *t*Bu), 1.48 (s, 9H; CH_3, *t*Bu), 1.76 (m, 2H; CH_2), 1.82 (s, 9H; CH_3, *t*Bu), 1.87 (s, 9H; CH_3, *t*Bu), 2.00 (m, 2H; CH_2–CH), 2.46 (m, 2H; CH_2–C=), 3.36 (m, 1H; CH), 4.48 (m, 1H; CH_2–O), 4.83 (m, 1H; CH_2–O), 7.2–8.2 ppm (m, 9H; CH=); ^{13}C NMR (C_6D_6): δ = 21.4 (CH_2), 23.9 (CH_2–C=), 26.1 (CH_2–CH), 31.8 (CH_3, *t*Bu), 35.0 (C, *t*Bu), 36.1 (C, *t*Bu), 39.1 (CH), 67.3 (CH_2–O), 125–165 ppm (aromatic carbon atoms); elemental analysis calcd (%) for $C_{42}H_{54}NO_3PS$: C 73.76, H 7.96, N 2.05; found: C 73.86, H 7.99, N 2.08.

Ligand L6b: Yield: 598 mg (48%); ^{31}P NMR (C_6D_6): δ = 137.5 ppm; ^{1}H NMR (C_6D_6): δ = 1.33 (m, 2H; CH_2), 1.54 (s, 9H; CH_3, *t*Bu), 1.59 (s, 9H; CH_3, *t*Bu), 1.82 (m, 2H; CH_2–CH), 2.27 (m, 2H; CH_2–C=), 3.15 (m, 1H; CH), 3.29 (s, 3H; CH_3–O), 3.33 (s, 3H; CH_3–O), 4.33 (m, 1H; CH_2–O), 4.71 (m, 1H; CH_2–O), 6.7–8.1 ppm (m, 9H; CH=); ^{13}C NMR (C_6D_6): δ = 21.7 (CH_2), 23.9 (CH_2–C=), 26.3 (CH_2–CH), 31.3 (CH_3, *t*Bu), 31.4 (CH_3, *t*Bu), 35.9 (C, *t*Bu), 36.0 (C, *t*Bu), 39.2 (CH), 55.4 (CH_3–O), 67.7 (CH_2–O), 112–165 ppm (aromatic carbon atoms); elemental analysis calcd (%) for $C_{36}H_{42}NO_5PS$: C 68.44, H 6.70, N 2.22; found: C 68.48, H 6.72, N 2.20.

Ligand L6c: Yield: 640 mg (53%); ^{31}P NMR (C_6D_6): δ = 136.5 ppm; ^{1}H NMR (C_6D_6): δ = 0.44 (s, 9H; CH_3–Si), 0.52 (s, 9H; CH_3–Si), 1.36 (m, 1H; CH_2), 1.56 (m, 1H; CH_2), 1.79 (m, 2H; CH_2–CH), 2.27 (m, 2H; CH_2–C=), 3.15 (m, 1H; CH), 4.15 (m, 1H; CH_2–O), 4.68 (m, 1H; CH_2–O), 6.9–8.2 ppm (m, 11H; CH=); ^{13}C NMR (C_6D_6): δ = 0.7 (CH_3–Si), 0.8 (CH_3–Si), 21.8 (CH_2), 24.2 (CH_2–C=), 26.5 (CH_2–CH), 39.3 (CH), 67.8 (CH_2–O), 125–165 ppm (aromatic carbon atoms); elemental analysis calcd (%) for $C_{32}H_{38}NO_3PSSi_2$: C 63.65, H 6.34, N 2.32; found: C 63.68, H 6.36, N 2.35.

Ligand L6d: Yield: 647 mg (47%); ^{31}P NMR (C_6D_6): δ = 136.2 ppm; ^{1}H NMR (C_6D_6): δ = 0.58 (s, 9H; CH_3–Si), 0.59 (s, 9H; CH_3–Si), 1.36 (m, 2H; CH_2), 1.72 (m, 2H; CH_2–CH), 2.32 (m, 2H; CH_2–C=), 2.94 (m, 1H; CH), 3.96 (m, 1H; CH_2–O), 4.76 (m, 1H; CH_2–O), 6.9–8.3 ppm (m, 15H; CH=); ^{13}C NMR (C_6D_6): δ = −0.3 (CH_3–Si), −0.1 (CH_3–Si), 21.3 (CH_2), 23.2 (CH_2–C=), 25.8 (CH_2–CH), 38.4 (d, *J*(C,P) = 3.2 Hz; CH), 67.1 (CH_2–O), 122–164 ppm (aromatic carbon atoms); elemental analysis calcd (%) for $C_{40}H_{42}NO_3PSSi_2$: C 68.24, H 6.01, N 1.99; found: C 68.21, H 5.98, N 1.97.

Ligand L6e: Yield: 605 mg (43%); ^{31}P NMR (C_6D_6): δ = 136.3 ppm; ^{1}H NMR (C_6D_6): δ = 0.61 (s, 9H; CH_3–Si), 0.73 (s, 9H; CH_3–Si), 1.31 (m, 1H; CH_2), 1.45 (m, 1H; CH_2), 1.63 (m, 1H; CH_2–CH), 1.88 (m, 1H; CH_2–CH), 2.16 (m, 2H; CH_2–C=), 3.21 (m, 1H; CH), 4.16 (m, 1H; CH_2–O), 4.43 (m, 1H; CH_2–O), 6.8–8.4 ppm (m, 15H; CH=); ^{13}C NMR (C_6D_6): δ = −0.2 (CH_3–Si), −0.1 (CH_3–Si), 20.6 (CH_2), 23.0 (CH_2–C=), 25.6 (CH_2–CH), 38.1 (d, *J*(C,P) = 4.0 Hz; CH), 67.1 (CH_2–O), 122–164 ppm (aromatic carbon atoms); elemental analysis calcd (%) for $C_{40}H_{42}NO_3PSSi_2$: C 68.24, H 6.01, N 1.99; found: C 68.27, H 6.03, N 2.02.

Ligand L7a: Yield: 598 mg (42%); ^{31}P NMR (C_6D_6): δ = 151.4 ppm; ^{1}H NMR (C_6D_6): δ = 1.19 (s, 3H; CH_3), 1.24 (s, 9H; CH_3, *t*Bu), 1.26 (s, 9H; CH_3, *t*Bu), 1.50 (s, 9H; CH_3, *t*Bu), 1.53 (s, 3H; CH_3), 1.62 (s, 9H; CH_3, *t*Bu), 1.89 (m, 2H; CH_2), 2.12 (m, 2H; CH_2–CH), 2.28 (m, 2H; CH_2–C=), 3.16 (m, 1H; CH), 7.0–8.0 ppm (m, 9H; CH=); ^{13}C NMR (C_6D_6): δ = 22.4 (CH_2), 24.3 (CH_2–C=), 26.4 (CH_2–CH), 27.9 (CH_3), 30.4 (CH_3), 31.4 (CH_3, *t*Bu), 31.6 (CH_3, *t*Bu), 31.8 (CH_3, *t*Bu), 35.1 (C, *t*Bu), 36.3 (C, *t*Bu), 36.4 (C, *t*Bu), 40.3 (CH), 71.0 (CMe_2), 124–166 ppm (aromatic carbon atoms); elemental analysis calcd (%) for $C_{44}H_{58}NO_3PS$: C 74.23, H 8.21, N 1.97; found: C 74.31, H 8.24, N 1.93.

Ligand L7d: Yield: 638 mg (42%); ^{31}P NMR (C_6D_6): δ = 143.2 ppm; ^{1}H NMR (C_6D_6): δ = 0.53 (s, 9H; CH_3–Si), 0.56 (s, 9H; CH_3–Si), 1.14 (s, 3H; CH_3), 1.50 (s, 3H; CH_3), 1.77 (m, 2H; CH_2), 2.09 (m, 2H; CH_2–CH), 2.25 (m, 2H; CH_2–C=), 3.17 (m, 1H; CH), 7.0–8.0 ppm (m, 15H; CH<C=>); ^{13}C NMR (C_6D_6): δ = −0.3 (CH_3–Si), −0.1 (CH_3–Si), 22.1 (CH_2), 23.8 (CH_2–C<C=>), 25.9 (CH_2–CH), 27.8 (CH_3), 29.9 (CH_3), 39.9 (CH), 70.3 (CH_2–O), 122–166 ppm (aromatic carbon atoms); elemental analysis calcd (%) for $C_{44}H_{50}NO_3PSSi_2$: C 69.53, H 6.63, N 1.84; found: C 69.55, H 6.64, N 1.80.

Ligand L8a: Yield: 798 mg (56%); ^{31}P NMR (C_6D_6): δ = 151.4 ppm; ^{1}H NMR (C_6D_6): δ = 1.24 (s, 9H; CH_3, *t*Bu), 1.26 (s, 9H; CH_3, *t*Bu), 1.50 (s, 9H; CH_3, *t*Bu), 1.53 (s, 3H; CH_3), 1.62 (s, 9H; CH_3, *t*Bu), 1.89 (m, 2H; CH_2), 2.12 (m, 2H; CH_2–CH), 2.28 (m, 2H; CH_2–C=), 3.16 (m, 1H; CH), 7.0–8.0 ppm (m, 9H; CH=); ^{13}C NMR (C_6D_6): δ = 22.4 (CH_2), 24.3 (CH_2–C=), 26.4 (CH_2–CH), 27.9 (CH_3), 30.4 (CH_3), 31.4 (CH_3, *t*Bu), 31.6 (CH_3, *t*Bu), 31.8 (CH_3, *t*Bu), 35.1 (C, *t*Bu), 36.3 (C, *t*Bu), 36.4 (C, *t*Bu), 40.3 (CH), 71.0 (CMe_2), 124–166 ppm (aromatic carbon atoms); elemental analysis calcd (%) for $C_{44}H_{58}NO_3PS$: C 74.23, H 8.21, N 1.97; found: C 74.28, H 8.21, N 1.99.

Ligand L8d: Yield: 808 mg (50%); ^{31}P NMR (C_6D_6): δ = 143.1 ppm; ^{1}H NMR (C_6D_6): δ = 0.49 (s, 9H; CH_3–Si), 0.59 (s, 9H; CH_3–Si), 1.19 (s, 3H; CH_3), 1.53 (s, 3H; CH_3), 1.74 (m, 2H; CH_2), 2.04 (m, 2H; CH_2–CH), 2.21 (m, 2H; CH_2–C=), 3.32 (m, 1H; CH), 7.0–8.0 ppm (m, 15H; CH=); ^{13}C NMR (C_6D_6): δ = −0.1 (CH_3–Si), 0.1 (CH_3–Si), 21.9 (CH_2), 23.4 (CH_2–C=), 26.3 (CH_2–CH), 27.9 (CH_3), 30.2 (CH_3), 39.3 (CH), 69.9 (CH_2–O), 122–166 ppm (aromatic carbon atoms); elemental analysis calcd (%) for $C_{44}H_{50}NO_3PSSi_2$: C 69.53, H 6.63, N 1.84; found: C 69.57, H 6.66, N 1.86.

General procedure for the preparation of [Pd(η^3-allyl)(L)]BF_4 complexes 26–35: The corresponding ligand (0.05 mmol) and the complex [{Pd(μ–Cl)(η^3-1,3-allyl)}$_2$] (0.025 mmol) were dissolved in CD_2Cl_2 (1.5 mL) at room temperature under argon. $AgBF_4$ (9.8 mg, 0.5 mmol) was added after 30 min and the mixture was stirred for 30 min. The mixture was then filtered over Celite under argon and the resulting solutions were analyzed by NMR spectroscopy. After the NMR spectroscopic analysis, the complexes were precipitated adding hexane as pale yellow solids.

Complex 26: Isomer **A** (90%): ^{31}P NMR (CD_2Cl_2, 263 K): δ = 135.6 ppm (s, 1P); ^{1}H NMR (CD_2Cl_2, 263 K): δ = 0.97 (s, 3H; CH_3), 1.05 (s, 3H; CH_3), 1.21 (s, 9H; CH_3, *t*Bu), 1.25 (s, 9H; CH_3, *t*Bu), 1.42 (s, 9H; CH_3, *t*Bu), 1.59 (s, 9H; CH_3, *t*Bu), 1.72 (m, 1H; CH_2), 1.84 (m, 1H; CH_2), 1.96 (m, 1H; CH_2–C=), 2.23 (m, 1H; CH_2–C=), 5.14 (m, 1H; CH allyl *trans* to N), 5.39 (m, 1H; CH–O), 5.99 (m, 1H; CH allyl *trans* to P), 6.55 (m, 1H; CH allyl central), 6.7–8.0 ppm (m, 19H; CH=); ^{13}C NMR (C_6D_6, 263 K): δ = 26.3 (CH_3), 29.8 (CH_3), 31.3 (CH_3, *t*Bu), 31.5 (CH_3, *t*Bu), 32.5 (C, *t*Bu), 34.8 (CH_2–C=), 35.6 (CMe_2), 42.5 (CH_2), 70.7 (br; CH–O), 81.4 (m; CH allyl *trans* to N), 95.9 (m; CH *trans* to P), 112.5 (m; CH allyl central), 125–164 ppm (aromatic carbon atoms). Isomer **B** (10%): ^{31}P NMR (CD_2Cl_2, 263 K): δ = 140.4 ppm (s, 1P); ^{1}H NMR (CD_2Cl_2, 263 K): δ = 0.99 (s, 3H; CH_3), 1.03 (s, 3H; CH_3), 1.14 (s, 9H; CH_3, *t*Bu), 1.17 (s, 9H; CH_3, *t*Bu), 1.40 (s, 9H; CH_3, *t*Bu), 1.55 (s, 9H; CH_3, *t*Bu), 1.85 (m, 1H; CH_2), 1.92 (m, 1H; CH_2–C=), 2.10 (m, 1H; CH_2–C=), 4.84 (m, 1H; CH allyl *trans* to N), 5.34 (m, 1H; CH–O), 5.21 (m, 1H; CH allyl *trans* to P), 6.45 (m, 1H; CH allyl central), 6.7–8.0 ppm (m, 19H; CH=); ^{13}C NMR (C_6D_6, 263 K): δ = 26.8 (CH_3), 30.1 (CH_3), 31.4 (CH_3, *t*Bu), 31.6 (CH_3, *t*Bu), 32.0 (C, *t*Bu), 35.1 (CH_2–C=), 35.8 (CMe_2), 42.3 (CH_2), 69.7 (br; CH–O), 75.0 (m; CH allyl *trans* to N), 95.4 (m; CH *trans* to P), 112.7 (m; CH allyl central), 125–164 ppm (aromatic carbon atoms); elemental analysis calcd (%) for $C_{58}H_{69}BF_4NO_4PPd$: C 65.20, H 6.51, N 1.31; found: C 65.43, H 6.61, N 1.35.

Complex 27: Isomer **A** (56%): ^{31}P NMR (CD_2Cl_2, 243 K): δ = 132.5 ppm (s, 1P); ^{1}H NMR (CD_2Cl_2, 243 K): δ = 1.45 (s, 9H; CH_3, *t*Bu), 1.49 (s, 9H; CH_3, *t*Bu), 1.65 (s, 9H; CH_3, *t*Bu), 1.69 (s, 9H; CH_3, *t*Bu), 1.82 (m, 2H; CH_2), 2.03 (m, 2H; CH_2–CH), 2.56 (m, 2H; CH_2–C=), 3.43 (m, 1H; CH), 4.56 (m, 1H; CH_2–O), 4.93 (m, 1H; CH allyl *trans* to N), 4.98 (m, 1H; CH_2–O), 5.87 (m, 1H; CH allyl *trans* to P), 6.33 (m, 1H; CH allyl central), 7.0–8.4 ppm (m, 19H; CH=); ^{13}C NMR (CD_2Cl_2, 243 K): δ = 22.1 (CH_2), 24.2 (CH_2–C=), 25.9 (CH_2–CH), 31.8–32.9 (br; CH_3, *t*Bu), 35.0 (C, *t*Bu), 35.8 (C, *t*Bu), 39.3 (CH), 69.1 (CH_2–O), 80.4 (m; CH allyl *trans* to N), 98.3 (m; CH *trans* to P), 112.1 (m; CH allyl central), 125–165 ppm (aromatic carbon atoms). Isomer **B** (44%): ^{31}P NMR (CD_2Cl_2, 243 K): δ = 136.9 ppm (s, 1P); ^{1}H NMR (CD_2Cl_2, 243 K): δ = 1.42 (s, 9H; CH_3, *t*Bu), 1.52 (s, 9H; CH_3, *t*Bu), 1.72 (s, 18H; CH_3, *t*Bu), 1.89 (m, 2H; CH_2), 2.12 (m, 2H; CH_2–CH), 2.63 (m, 2H; CH_2–C=), 3.49 (m, 1H; CH), 4.53 (m, 1H; CH_2–O), 4.88 (m, 1H; CH allyl *trans* to N), 5.13 (m, 1H; CH_2–O), 5.45 (m, 1H; CH allyl *trans* to P), 6.28 (m, 1H; CH allyl central), 7.0–8.4 ppm (m, 19H; CH=); ^{13}C NMR (CD_2Cl_2, 243 K): δ = 22.3 (CH_2), 24.5 (CH_2–C=), 26.1 (CH_2–CH), 31.8–32.9 (br; CH_3, *t*Bu), 35.3 (C, *t*Bu), 35.5 (C, *t*Bu), 39.2 (CH), 70.0 (CH_2–O), 77.2 (m; CH allyl *trans* to N), 96.2 (m; CH *trans* to P), 112.0 (m; CH allyl central), 125–165 ppm (aromatic carbon atoms); elemental analysis calcd (%) for $C_{57}H_{67}BF_4NO_3PPdS$: C 63.96, H 6.31, N 1.31; found: C 64.03, H 6.32, N 1.33.

Complex 28: Isomer **A** (70%): ^{31}P NMR (CD_2Cl_2, 233 K): δ = 139.2 ppm (s, 1P); ^{1}H NMR (CD_2Cl_2, 233 K): δ = 0.62 (s, 3H; CH_3), 0.89 (s, 3H; CH_3), 1.31 (s, 18H; CH_3, *t*Bu), 1.43 (s, 9H; CH_3, *t*Bu), 1.54 (s, 9H; CH_3, *t*Bu), 1.69 (m, 1H; CH_2), 1.74 (s, 9H; CH_3, *t*Bu), 1.86 (m, 1H; CH_2), 2.01 (m, 1H; CH_2–C=), 2.24 (m, 1H; CH_2–C=), 5.43 (m, 1H; CH allyl *trans* to N), 5.57 (m, 1H; CH–O), 6.02 (m, 1H; CH allyl *trans* to P), 6.21 (m, 1H; CH allyl central), 6.8–8.0 ppm (m, 14H; CH=); ^{13}C NMR (CD_2Cl_2, 233 K): δ = 28.1 (CH_3), 29.4 (CH_3), 30.2–32.5 (CH_3, *t*Bu), 33.5 (CMe_2), 34.5 (C, *t*Bu), 34.7 (C, *t*Bu), 35.2 (C, *t*Bu), 36.2 (CH_2–C=), 36.4 (C, *t*Bu), 45.5 (CH_2), 68.4 (m; CH–O), 81.4 (m; CH allyl *trans* to N), 95.9 (m; CH *trans* to P), 112.3 (m; CH allyl central), 124–170 ppm (aromatic carbon atoms). Product **C** (30%): ^{31}P NMR (CD_2Cl_2, 233 K): δ = 143.1 ppm (s, 1P); ^{1}H NMR (CD_2Cl_2, 233 K): δ = 0.59 (s, 6H; CH_3), 0.84 (s, 6H; CH_3), 1.29 (s, 18H; CH_3, *t*Bu), 1.33 (s, 18H; CH_3, *t*Bu), 1.59 (s, 36H; CH_3, *t*Bu), 1.64 (m, 2H; CH_2), 1.71 (s, 18H; CH_3, *t*Bu), 1.81 (m, 2H; CH_2), 2.06 (m, 2H; CH_2–C=), 2.18 (m, 2H; CH_2–C=), 5.32 (m, 1H; CH allyl), 5.52 (m, 2H; CH–O), 5.59 (m, 1H; CH allyl), 6.19 (m, 1H; CH allyl central), 6.8–8.0 ppm (m, 18H; CH=); ^{13}C NMR (CD_2Cl_2, 233 K): δ = 28.2 (CH_3), 29.6 (CH_3), 30.2-32.5 (CH_3, *t*Bu), 33.7 (CMe_2), 34.3 (C, *t*Bu), 34.9 (C, *t*Bu), 35.0 (C, *t*Bu), 35.5 (C, *t*Bu), 36.3 (CH_2–C=), 36.9 (C, *t*Bu), 45.3 (CH_2), 69.2 (m; CH–O), 99.7 (br; CH allyl), 112.5 (m; CH allyl central), 124–170 ppm (aromatic carbon atoms); elemental analysis calcd (%) for $0.7\,C_{56}H_{73}BF_4NO_4PPd + 0.3\,C_{97}H_{133}BF_4N_2O_8P_2Pd$: C 65.79, H 7.36, N 0.87; found: C 65.87, H 7.42, N 0.92.

Complex 29: Isomer **A** (83%): ^{31}P NMR (CD_2Cl_2, 273 K): δ = 138.1 ppm (s, 1P); ^{1}H NMR (C_6D_6, 273 K): δ = 0.22 (s, 9H; CH_3–Si), 0.75 (s, 9H; CH_3–Si), 1.04 (s, 3H; CH_3), 1.18 (s, 3H; CH_3), 1.92 (m, 1H; CH_2), 2.21 (m, 1H; CH_2), 2.53 (m, 2H; CH_2–C=), 4.97 (m, 1H; CH allyl *trans* to N), 5.38 (m, 1H; CH–O), 6.06 (m, 1H; CH allyl *trans* to P), 6.42 (m, 1H; CH allyl central), 6.6–8.3 ppm (m, 25H; CH=); ^{13}C NMR (C_6D_6, 273 K): δ = 0.7 (CH_3–Si), 1.0 (CH_3–Si), 28.2 (CH_3), 32.9 (CMe_2), 35.2 (CH_2–C=), 42.5 (d, J(C,P) = 1.2 Hz; CH_2), 70.5 (d, J(C,P) = 7.2 Hz; CH–O), 75.4 (m; CH allyl *trans* to N), 96.7 (m; CH allyl *trans* to P), 112.4 (m; CH allyl central), 121–165 ppm (aromatic carbon atoms). Isomer **B** (17%): ^{31}P NMR (CD_2Cl_2, 273 K): δ = 140.5 ppm (s, 1P); ^{1}H NMR (C_6D_6, 273 K): δ = 0.56 (s, 9H; CH_3–Si), 0.69 (s, 9H; CH_3–Si), 1.04 (s, 3H; CH_3), 1.07 (s, 3H; CH_3), 1.70 (m, 1H; CH_2), 1.98 (m, 1H; CH_2), 2.21 (m, 2H; CH_2–C=), 5.19 (m, 1H; CH allyl *trans* to N), 5.32 (m, 1H; CH allyl *trans* to P), 5.42 (m, 1H; CH–O), 6.49 (m, 1H; CH allyl central), 6.6–8.3 ppm (m, 25H; CH=); ^{13}C NMR (C_6D_6, 273 K): δ = 1.2 (CH_3–Si), 1.5 (CH_3–Si), 26.3 (CH_3), 29.5 (CH_3), 33.4 (CMe_2), 35.0 (CH_2–C=), 42.7 (d, J(C,P) = 3.2 Hz; CH_2), 68.5 (d, J(C,P) = 7.2 Hz; CH–O), 70.7 (m; CH allyl *trans* to N), 96.1 (m; CH allyl *trans* to P), 110.7 (m; CH allyl central), 121–165 ppm (aromatic carbon atoms); elemental analysis calcd (%) for $C_{56}H_{57}BF_4NO_4PPdSi_2$: C 61.80, H 5.28, N 1.29; found: C 61.92, H 5.34, N 1.33.

Complex 30: Isomer **A** (28%): ^{31}P NMR (CD_2Cl_2, 223 K): δ = 140.6 ppm (s, 1P); ^{1}H NMR (C_6D_6, 223 K): δ = 0.04 (s, 9H; CH_3–Si), 0.65 (s, 9H; CH_3–Si), 0.98 (s, 3H; CH_3), 1.20 (s, 3H; CH_3), 1.64 (m, 1H; CH_2), 2.03 (m, 1H; CH_2), 2.54 (m, 2H; CH_2–C=), 4.80 (m, 1H; CH allyl *trans* to N), 5.33 (m, 1H; CH–O), 5.77 (m, 1H; CH allyl *trans* to P), 6.17 (m, 1H; CH allyl central), 6.4–8.4 ppm (m, 25H; CH=); ^{13}C NMR (C_6D_6, 223 K): δ = −0.5 (CH_3–Si), 1.1 (CH_3–Si), 25.1 (CH_3), 30.2 (CH_3), 33.5 (CMe_2), 34.8 (CH_2–C=), 42.6 (d, J(C,P) = 10.2 Hz; CH_2), 69.3 (CH–O), 71.1 (d, J(C,P) = 8.0 Hz; CH allyl *trans* to N), 98.4 (m; CH allyl *trans* to P), 110.9 (m; CH allyl central), 120–165 ppm (aromatic carbon atoms). Isomer **B** (72%): ^{31}P NMR (CD_2Cl_2, 223 K): δ = 141.1 ppm (s, 1P); ^{1}H NMR (C_6D_6, 223 K): δ = 0.25 (s, 9H; CH_3–Si), 0.69 (s, 9H; CH_3–Si), 1.07 (s, 3H; CH_3), 1.14 (s, 3H; CH_3), 1.67 (m, 1H; CH_2), 2.18 (m, 1H; CH_2), 2.62 (m, 2H; CH_2–C=), 4.74 (m, 1H; CH allyl *trans* to N), 5.30 (m, 1H; CH allyl *trans* to P), 5.37 (m, 1H; CH–O), 6.21 (m, 1H; CH allyl central), 6.4–8.4 ppm (m, 25H; CH=); ^{13}C NMR (C_6D_6, 223 K): δ = 0.3 (CH_3–Si), 1.4 (CH_3–Si), 25.2 (CH_3), 30.8 (CH_3), 33.5 (CMe_2), 34.8 (CH_2–C=), 43.0 (d, J(C,P) =

9.4 Hz; CH_2), 69.2 (CH−O), 70.5 (d, J(C,P) = 9.6 Hz; CH allyl *trans* to N), 93.0 (d, J(C,P) = 36.8 Hz; CH allyl *trans* to P), 111.2 (m; CH allyl central), 120–165 ppm (aromatic carbon atoms); elemental analysis calcd (%) for $C_{56}H_{57}BF_4NO_4PPdSi_2$: C 61.80, H 5.28, N 1.29; found: C 61.91, H 5.37, N 1.34.

Complex 31: Isomer **A** (46%): ^{31}P NMR (CD_2Cl_2, 295 K): δ = 134.3 ppm (s, 1P); ^{1}H NMR (CD_2Cl_2, 295 K): δ = 0.84 (m, 3H; CH_3 allyl), 1.12 (m, 3H; CH_3 allyl), 1.15 (s, 3H; CH_3), 1.29 (s, 3H; CH_3), 1.35 (s, 9H; CH_3, *t*Bu), 1.39–1.42 (s, 18H; CH_3, *t*Bu), 1.59 (s, 9H; CH_3, *t*Bu), 1.95 (m, 1H; CH_2), 2.35 (m, 1H; CH_2), 2.69 (m, 1H; CH_2−C=), 2.73 (m, 1H; CH_2−C=), 4.12 (m, 1H; CH allyl *trans* to N), 5.03 (m, 1H; CH allyl *trans* to P), 5.36 (m, 1H; CH allyl central), 5.46 (m, 1H; CH−O), 7.1–8.1 ppm (m, 9H; CH=); ^{13}C NMR (CD_2Cl_2, 295 K): δ = 16.3 (CH_3 allyl), 19.4 (CH_3 allyl), 26.8 (CH_3), 29.9 (CH_3), 31.4–32.1 (CH_3, *t*Bu), 32.5–33.6 (C, *t*Bu), 35.2 (CH_2−C=), 36.0 (CMe_2), 42.9 (br; CH_2), 70.6 (br; CH−O), 72.3 (m; CH allyl *trans* to N), 107.3 (m; CH *trans* to P), 115.3 (m; CH allyl central), 123–164 ppm (aromatic carbon atoms). Isomer **B** (18%): ^{31}P NMR (CD_2Cl_2, 295 K): δ = 135.2 ppm (s, 1P); ^{1}H NMR (CD_2Cl_2, 295 K): δ = 0.90 (m, 3H; CH_3 allyl), 1.05 (m, 3H; CH_3 allyl), 1.18 (s, 3H; CH_3), 1.28 (s, 3H; CH_3), 1.39–1.42 (s, 18H; CH_3, *t*Bu), 1.49 (s, 9H; CH_3, *t*Bu), 1.53 (s, 9H; CH_3, *t*Bu), 1.98 (m, 1H; CH_2), 2.22 (m, 1H; CH_2), 2.73 (m, 1H; CH_2−C=), 2.78 (m, 1H; CH_2−C=), 4.50 (m, 1H; CH allyl *trans* to N), 4.73 (m, 1H; CH allyl *trans* to P), 5.42 (m, 1H; CH allyl central), 5.52 (m, 1H; CH−O), 7.1–8.1 ppm (m, 9H; CH=); ^{13}C NMR (CD_2Cl_2, 295 K): δ = 16.2 (CH_3 allyl), 17.5 (CH_3 allyl), 27.3 (CH_3), 29.4 (CH_3), 31.4-32.1 (CH_3, *t*Bu), 32.5-33.6 (C, *t*Bu), 35.4 (CH_2−C=), 36.3 (CMe_2), 42.9 (br; CH_2), 70.2 (br; CH−O), 74.5 (m; CH allyl *trans* to N), 106.3 (m; CH *trans* to P), 116.8 (m; CH allyl central), 123–164 ppm (aromatic carbon atoms). Isomer **D** (36%): ^{31}P NMR (CD_2Cl_2, 295 K): δ = 134.7 ppm (s, 1P); ^{1}H NMR (CD_2Cl_2, 295 K): δ = 0.54 (m, 3H; CH_3 allyl), 0.95 (m, 3H; CH_3 allyl), 1.20 (s, 3H; CH_3), 1.22 (s, 3H; CH_3), 1.39–1.42 (s, 9H; CH_3, *t*Bu), 1.45 (s, 9H; CH_3, *t*Bu), 1.54 (s, 9H; CH_3, *t*Bu), 1.60 (s, 9H; CH_3, *t*Bu), 1.98 (m, 1H; CH_2), 2.20 (m, 1H; CH_2), 2.78 (m, 1H; CH_2−C=), 2.82 (m, 1H; CH_2−C=), 3.61 (m, 1H; CH allyl *trans* to N), 3.87 (m, 1H; CH allyl *trans* to P), 5.23 (m, 1H; CH allyl central), 5.71 (m, 1H; CH−O), 7.1–8.1 ppm (m, 9H; CH=); ^{13}C NMR (CD_2Cl_2, 295 K): δ = 17.5 (CH_3 allyl), 18.8 (CH_3 allyl), 27.5 (CH_3), 29.4 (CH_3), 31.4–32.1 (CH_3, *t*Bu), 32.5–33.6 (C, *t*Bu), 35.5 (CH_2−C=), 36.2 (CMe_2), 42.9 (br; CH_2), 69.8 (br; CH−O), 70.6 (m; CH allyl *trans* to N), 95.0 (m; CH *trans* to P), 118.6 (m; CH allyl central), 123–164 ppm (aromatic carbon atoms); elemental analysis calcd (%) for $C_{48}H_{65}BF_4NO_4PPd$: C 61.06, H 6.94, N 1.48; found: C 61.11, H 6.96, N 1.49.

Complex 32: Isomer **A** (40%): ^{31}P NMR (CD_2Cl_2, 253 K): δ = 127.4 ppm (s, 1P); ^{1}H NMR (CD_2Cl_2, 253 K): δ = 0.63 (m, 3H; CH_3 allyl), 0.85 (m, 3H; CH_3 allyl), 1.19 (s, 3H; CH_3), 1.26 (s, 3H; CH_3), 1.37 (s, 9H; CH_3, *t*Bu), 1.39 (s, 9H; CH_3, *t*Bu), 1.44 (s, 9H; CH_3, *t*Bu), 1.51 (s, 9H; CH_3, *t*Bu), 1.85 (m, 2H; CH_2), 2.06 (m, 2H; CH_2−CH), 2.22 (m, 2H; CH_2−C=), 2.73 (m, 1H; CH_2−C=), 3.42 (m, 1H; CH allyl *trans* to N), 4.26 (m, 1H; CH−O), 4.56 (m, 1H; CH allyl *trans* to P), 4.91 (m, 1H; CH allyl central), 7.1–8.2 ppm (m, 9H; CH=); ^{13}C NMR (CD_2Cl_2, 253 K): δ = 17.0 (CH_3 allyl), 18.1 (CH_3 allyl), 21.0 (CH_2), 23.8 (CH_2−C=), 26.0 (CH_2−CH), 26.1 (CH_3), 29.5 (CH_3), 31.4–32.2 (CH_3, *t*Bu), 35.1–36.2 (C, *t*Bu), 46.5 (CH), 64.8 (m; CH allyl *trans* to N), 78.3(CMe_2), 107.8 (m; CH *trans* to P), 115.8 (m; CH allyl central), 125–170 ppm (aromatic carbon atoms). Isomer **B** (8%): ^{31}P NMR (CD_2Cl_2, 253 K): δ = 129.1 ppm (s, 1P); ^{1}H NMR (CD_2Cl_2, 253 K): δ = 0.53 (m, 3H; CH_3 allyl), 0.74 (m, 3H; CH_3 allyl), 1.15 (s, 3H; CH_3), 1.31 (s, 3H; CH_3), 1.32 (s, 9H; CH_3, *t*Bu), 1.53 (s, 9H; CH_3, *t*Bu), 1.62 (s, 9H; CH_3, *t*Bu), 1.71 (s, 9H; CH_3, *t*Bu), 1.87 (m, 2H; CH_2), 2.06 (m, 2H; CH_2−CH), 2.22 (m, 2H; CH_2−C=), 2.73 (m, 1H; CH_2−C=), 3.48 (m, 1H; CH allyl *trans* to N), 3.71 (m, 1H; CH allyl *trans* to P), 4.11 (m, 1H; CH−O), 5.07 (m, 1H; CH allyl central), 7.1–8.2 ppm (m, 9H; CH=); ^{13}C NMR (CD_2Cl_2, 253 K): δ = 17.2 (CH_3 allyl), 18.6 (CH_3 allyl), 20.7 (CH_2), 23.8 (CH_2−C=), 25.7 (CH_2−CH), 26.8 (CH_3), 29.1 (CH_3), 31.4–32.2 (CH_3, *t*Bu), 35.1–36.2 (C, *t*Bu), 46.7 (CH), 65.7 (m; CH allyl *trans* to N), 78.1 (CMe_2), 106.7 (m; CH *trans* to P), 115.9 (m; CH allyl central), 125–170 ppm (aromatic carbon atoms). Isomer **D** (52%): ^{31}P NMR (CD_2Cl_2, 253 K): δ = 128.0 ppm (s, 1P); ^{1}H NMR (CD_2Cl_2, 253 K): δ = 0.59 (m, 3H; CH_3 allyl), 0.88 (m, 3H; CH_3 allyl), 1.09 (s, 3H; CH_3), 1.21 (s, 3H; CH_3), 1.35 (s, 9H; CH_3, *t*Bu), 1.46 (s, 9H; CH_3, *t*Bu), 1.50 (s, 9H; CH_3, *t*Bu), 1.78 (s, 9H; CH_3, *t*Bu), 1.94 (m, 2H; CH_2), 2.06 (m, 2H; CH_2−CH), 2.22 (m, 2H; CH_2−C=), 2.73 (m, 1H; CH_2−C=), 3.18 (m, 1H; CH allyl *trans* to N), 3.83 (m, 1H; CH allyl *trans* to P), 4.05 (m, 1H; CH−O), 4.89 (m, 1H; CH allyl central), 7.1–8.2 ppm (m, 9H; CH=); ^{13}C NMR (CD_2Cl_2, 253 K): δ = 18.0 (CH_3 allyl), 18.3 (CH_3 allyl), 21.1 (CH_2), 23.8 (CH_2−C=), 25.9 (CH_2−CH), 26.7 (CH_3), 30.2 (CH_3), 31.4-32.2 (CH_3, *t*Bu), 35.1–36.2 (C, *t*Bu), 46.5 (CH), 66.8 (m; CH allyl *trans* to N), 78.2 (CMe_2), 95.4 (m; CH *trans* to P), 115.7 (m; CH allyl central), 125–170 ppm (aromatic carbon atoms); elemental analysis calcd (%) for $C_{49}H_{67}BF_4NO_3PPdS$: C 60.40, H 6.93, N 1.44; found: C 60.37, H 6.90, N 1.43.

Complex 33: Isomer **A** (45%): ^{31}P NMR (CD_2Cl_2, 253 K): δ = 132.2 ppm (s, 1P); ^{1}H NMR (CD_2Cl_2, 253 K): δ = 0.42 (m, 9H; CH_3−Si), 0.60 (m, 9H; CH_3−Si), 0.68 (m, 3H; CH_3 allyl), 0.87 (m, 3H; CH_3 allyl), 1.21 (s, 3H; CH_3), 1.28 (s, 3H; CH_3), 1.84 (m, 2H; CH_2), 2.11 (m, 2H; CH_2−CH), 2.24 (m, 2H; CH_2−C=), 2.69 (m, 1H; CH_2−C=), 3.89 (m, 1H; CH allyl *trans* to N), 4.13 (m, 1H; CH−O), 4.26 (m, 1H; CH allyl *trans* to P), 4.98 (m, 1H; CH allyl central), 7.0–8.4 ppm (m, 15H; CH=); ^{13}C NMR (CD_2Cl_2, 253 K): δ = 0.8 (CH_3−Si), 1.4 (CH_3−Si), 16.5 (CH_3 allyl), 19.4 (CH_3 allyl), 21.5 (CH_2), 24.2 (CH_2−C=), 26.3 (CH_2−CH), 26.6 (CH_3), 29.9 (CH_3), 45.8 (CH), 73.1 (m; CH allyl *trans* to N), 76.4 (CMe_2), 104.3 (m; CH *trans* to P), 115.3 (m; CH allyl central), 125–170 ppm (aromatic carbon atoms). Isomer **B** (5%): ^{31}P NMR (CD_2Cl_2, 253 K): δ = 136.3 ppm (s, 1P); ^{1}H NMR (CD_2Cl_2, 253 K): δ = 0.39 (m, 9H; CH_3−Si), 0.57 (m, 9H; CH_3−Si), 0.74 (m, 3H; CH_3 allyl), 1.04 (m, 3H; CH_3 allyl), 1.24 (s, 3H; CH_3), 1.31 (s, 3H; CH_3), 1.86 (m, 2H; CH_2), 2.11 (m, 2H; CH_2−CH), 2.24 (m, 2H; CH_2−C=), 2.69 (m, 1H; CH_2−C=), 3.90 (m, 1H; CH allyl *trans* to N), 4.10 (m, 1H; CH−O), 4.15 (m, 1H; CH allyl *trans* to P), 4.95 (m, 1H; CH allyl central), 7.0–8.4 ppm (m, 15H; CH=); ^{13}C NMR (CD_2Cl_2, 253 K): δ = 0.5 (CH_3−Si), 1.2 (CH_3−Si), 16.2 (CH_3 allyl), 19.4 (CH_3 allyl), 21.6 (CH_2), 24.1 (CH_2−C=), 26.2 (CH_2−CH), 26.7 (CH_3), 30.1 (CH_3), 45.6 (CH), 74.0 (m; CH allyl *trans* to N), 76.3 (CMe_2), 102.1 (m; CH *trans* to P), 116.1 (m; CH allyl central), 125–170 ppm (aromatic carbon atoms). Isomer **D** (50%): ^{31}P NMR (CD_2Cl_2, 253 K): δ = 134.6 ppm (s, 1P); ^{1}H NMR (CD_2Cl_2, 253 K): δ = 0.51 (m, 9H; CH_3−Si), 0.58 (m, 9H; CH_3−Si), 0.75 (m, 3H; CH_3 allyl), 0.82 (m, 3H; CH_3 allyl), 1.27 (s, 3H; CH_3), 1.41 (s, 3H; CH_3), 1.84 (m, 2H; CH_2), 2.11 (m, 2H; CH_2−CH), 2.24 (m, 2H; CH_2−C=), 2.69 (m, 1H; CH_2−C=), 3.64 (m, 1H; CH allyl *trans* to N), 3.98 (m, 1H; CH allyl *trans* to P), 4.18 (m, 1H; CH−O), 4.79 (m, 1H; CH allyl central), 7.0–8.4 ppm (m, 15H; CH=); ^{13}C NMR (CD_2Cl_2, 253 K): δ = 0.9 (CH_3−Si), 1.0 (CH_3−Si), 16.4 (CH_3 allyl), 19.2 (CH_3 allyl), 21.7 (CH_2), 24.0 (CH_2−C=), 26.1 (CH_2−CH), 26.9 (CH_3), 30.2 (CH_3), 45.9 (CH), 71.3 (m; CH allyl *trans* to N), 76.3 (CMe_2), 96.1 (m; CH *trans* to P), 115.5 (m; CH allyl central), 125–170 ppm (aromatic carbon atoms); elemental analysis calcd (%) for $C_{47}H_{55}BF_4NO_3PPdSSi_2$: C 56.77, H 5.58, N 1.41; found: C 56.73, H 5.55, N 1.38.

Complex 34: Isomer **A** (15%): ^{31}P NMR (CD_2Cl_2): δ = 139.1 ppm (s, 1P); ^{1}H NMR (CD_2Cl_2): δ = 0.32 (s, 9H; CH_3−Si), 0.44 (s, 9H; CH_3−Si), 1.09 (s, 3H; CH_3), 1.16 (m, 3H; CH_3), 1.39 (m, 2H; CH_2, allyl), 1.49 (m, 2H; CH_2), 1.72 (m, 4H; CH_2 allyl), 1.92 (m, 1H; CH_2−CH), 2.14 (m, 1H; CH_2−CH), 2.72 (CH_2−C=), 4.94 (m, 1H; CH allyl *trans* to N), 5.49 (m, 1H; CH−O), 5.79 (m, 1H; CH allyl central), 5.98 (m, 1H; CH allyl *trans* to P), 6.8–8.4 ppm (m, 15H; CH=); ^{13}C NMR (CD_2Cl_2): δ = 0.3 (CH_3−Si), 19.1 (CH_2 allyl), 26.3 (CH_2 allyl), 28.2 (CH_3), 28.7 (CH_3), 31.0 (CH_2 allyl), 33.0 (CMe_2), 35.5 (CH_2−C=), 42.2 (m; CH_2), 69.7 (CH−O), 70.6 (m; CH allyl *trans* to N), 103.2 (d, J(C,P) = 38.2 Hz; CH allyl *trans* to P), 112.7 (m; CH allyl central), 121–167 ppm (aromatic carbon atoms). Isomer **B** (85%): ^{31}P NMR (CD_2Cl_2): δ = 138.7 ppm (s, 1P); ^{1}H NMR (CD_2Cl_2): δ = 0.37 (s, 9H; CH_3−Si), 0.52 (s, 9H; CH_3−Si), 0.94 (m, 2H; CH_2, allyl), 1.14 (s, 3H; CH_3), 1.23 (s, 3H; CH_3), 1.42 (m, 4H; CH_2 and CH_2 allyl), 1.62 (m, 2H; CH_2 allyl), 2.03 (m, 1H; CH_2−CH), 2.26 (m, 1H; CH_2−CH), 2.75 (CH_2−C=), 3.72 (m, 1H; CH allyl *trans* to N), 5.30 (m, 1H; CH allyl central), 5.42 (m, 1H; CH allyl *trans* to P), 5.52 (m, 1H; CH−O), 6.8–8.4 ppm (m, 15H; CH=); ^{13}C NMR (CD_2Cl_2): δ = 0.9 (CH_3−Si), 1.1 (CH_3−Si), 20.2 (CH_2 allyl), 25.5 (CH_2 allyl), 26.5 (CH_3), 29.1 (CH_3), 30.9 (CH_2 allyl), 33.6 (CMe_2), 35.5 (CH_2−C=), 43.7 (CH_2), 69.9 (m; CH−O), 70.4 (m; CH allyl *trans* to N), 106.2 (d, J(C,P) = 38.2 Hz; CH allyl *trans* to P), 111.3 (m; CH allyl central), 121–167 ppm

(aromatic carbon atoms); elemental analysis calcd (%) for $C_{47}H_{53}BF_4NO_4PPdSi_2$: C 57.82, H 5.47, N 1.43; found: C 57.91, H 5.51, N 1.45.

Complex 35: Isomer **A** (87%): ^{31}P NMR (CD_2Cl_2): $\delta = 141.6$ ppm (s, 1P); ^{1}H NMR (CD_2Cl_2): $\delta = 0.53$ (s, 9H; CH_3–Si), 0.56 (s, 9H; CH_3–Si), 0.89 (m, 2H; CH_2, allyl), 1.15 (s, 3H; CH_3), 1.21 (m, 2H; CH_2, allyl), 1.32 (s, 3H; CH_3), 1.36 (m, 2H; CH_2), 1.45 (m, 2H; CH_2 allyl), 1.96 (m, 1H; CH_2–CH), 2.17 (m, 1H; CH_2–CH), 2.72 (CH_2–C=), 3.87 (m, 1H; CH allyl *trans* to N), 5.21 (m, 1H; CH allyl central), 5.32 (m, 1H; CH–O), 5.36 (m, 1H; CH allyl *trans* to P), 6.8–8.4 ppm (m, 15H; CH=); ^{13}C NMR (CD_2Cl_2): $\delta = 0.9$ (CH_3–Si), 1.1 (CH_3–Si), 20.2 (CH_2 allyl), 25.5 (CH_2 allyl), 26.5 (CH_3), 29.1 (CH_3), 30.9 (CH_2 allyl), 33.6 (CMe_2), 35.5 (CH_2–C=), 43.7 (CH_2), 68.6 (m; CH allyl *trans* to N), 69.9 (m; CH–O), 107.6 (d, J(C,P) = 38.2 Hz; CH allyl *trans* to P), 111.3 (m; CH allyl central), 121–167 ppm (aromatic carbon atoms). Isomer **B** (13%): ^{31}P NMR (CD_2Cl_2): $\delta = 140.3$ ppm (s, 1P); ^{1}H NMR (CD_2Cl_2): $\delta = 0.54$ (s, 9H; CH_3–Si), 0.59 (s, 9H; CH_3–Si), 1.16 (s, 3H; CH_3), 1.24 (m, 4H; CH_3 and CH_2 allyl), 1.49 (m, 1H; CH_2 allyl), 1.67 (m, 1H; CH_2–CH), 1.93 (m, 1H; CH_2 allyl), 2.08 (m, 1H; CH_2–CH), 2.72 (CH_2–C=), 4.69 (m, 1H; CH allyl *trans* to N), 4.84 (m, 1H; CH–O), 5.18 (m, 1H; CH allyl *trans* to P), 5.41 (m, 1H; CH allyl central), 6.8–8.4 ppm (m, 15H; CH=); ^{13}C NMR (CD_2Cl_2): $\delta = 1.2$ (CH_3–Si), 1.6 (CH_3–Si), 20.2 (CH_2 allyl), 25.5 (CH_2 allyl), 26.6 (CH_3), 29.2 (CH_3), 30.8 (CH_2 allyl), 33.4 (CMe_2), 35.5 (CH_2–C=), 45.6 (CH_2), 62.4 (m; CH–O), 68.6 (m; CH allyl *trans* to N), 104.7 (d, J(C,P) = 34.6 Hz; CH allyl *trans* to P), 112.4 (m; CH allyl central), 121–167 ppm (aromatic carbon atoms); elemental analysis calcd (%) for $C_{47}H_{53}BF_4NO_4PPdSi_2$: C 57.82, H 5.47, N 1.43; found: C 57.87, H 5.49, N 1.44.

Study of the reactivity of the [Pd(η^3-allyl)(L)]BF_4 with sodium malonate by in situ NMR spectroscopy:[37] A solution of in situ prepared [Pd(η^3-allyl)(L)]BF_4 (L = phosphite–nitrogen ligand, 0.05 mmol) in CD_2Cl_2 (1 mL) was cooled in the NMR spectroscopy tube at −80°C. At this temperature, a solution of cooled sodium malonate (0.1 mmol) was added. The reaction was then followed by ^{31}P NMR spectroscopy. The relative reaction rates were calculated using a capillary containing a solution of triphenylphosphine in CD_2Cl_2 as external standard.

Typical procedure of allylic alkylation of disubstituted linear (S1 and S3) and cyclic (S4–S6) substrates: A degassed solution of [PdCl(η^3–C_3H_5)]$_2$ (0.9 mg, 0.0025 mmol) and the corresponding phosphite–nitrogen ligand (0.0055 mmol) in dichloromethane (0.5 mL) was stirred for 30 min. Subsequently, a solution of the corresponding substrate (0.5 mmol) in dichloromethane (1.5 mL), dimethyl malonate (171 µL, 1.5 mmol), *N,O*-bis(trimethylsilyl)acetamide (370 µL, 1.5 mmol), and the corresponding base (5 mg) were added. The reaction mixture was stirred at room temperature. After the desired reaction time, the reaction mixture was diluted with Et_2O (5 mL) and saturated aqueous NH_4Cl (25 mL) was added. The mixture was extracted with Et_2O (3×10 mL) and the extract dried over $MgSO_4$. For substrate **S1**, solvent was removed and conversion was measured by ^{1}H NMR spectroscopy. To determine the *ee* by HPLC (Chiralcel OD, 0.5% 2-propanol/hexane, flow 0.5 mL min^{-1}), a sample was filtered over basic alumina using dichloromethane as the eluent.[38] For substrates **S3–S6**, conversion and enantiomeric excess were determined by GC.[24]

Typical procedure of allylic alkylation of disubstituted linear (S2), 1,3,3-trisubstituted (S7 and S8), and monosubstituted (S9 and S10) substrates: A degassed solution of [{PdCl(η^3–C_3H_5)}$_2$] (1.8 mg, 0.005 mmol) and the corresponding phosphite–nitrogen ligand (0.011 mmol) in dichloromethane (0.5 mL) was stirred for 30 min at room temperature. Subsequently, a solution of substrate (0.5 mmol) in dichloromethane (1.5 mL), dimethyl malonate (171 µL, 1.5 mmol), *N,O*-bis(trimethylsilyl)acetamide (370 µL, 1.5 mmol), and KOAc (5 mg) were added. After 2 h at room temperature, the reaction mixture was diluted with Et_2O (5 mL) and saturated aqueous NH_4Cl (25 mL) was added. The mixture was extracted with Et_2O (3×10 mL) and the extract dried over $MgSO_4$. Solvent was removed and conversion and regioselectivity were measured by ^{1}H NMR spectroscopy. For substrate **S2**, enantiomeric excess was determined by ^{1}H NMR spectroscopy using [Eu(hfc)$_3$] as resolving agent (hfc = 6,6,7,7,8,8,8-heptafluoro-2,2′-dimethyl-1,3,5- hydroxymethylene(+) camphore).[15b] For substrates **S7** and **S8**, to determine the *ee* by HPLC (Chiralcel OJ, 13% 2-propanol/hexane, flow 0.5 mL min^{-1}), a sample was filtered over basic alumina using dichloromethane as the eluent.[24] For substrates **S9** and **S10**, to determine the *ee* by HPLC (Chiralcel OJ, 13% 2-propanol/hexane, flow 0.7 mL min^{-1}), a sample was filtered over basic alumina using dichloromethane as the eluent.[39]

Typical procedure of allylic amination of disubstituted linear substrate S1: A degassed solution of [{PdCl(η^3–C_3H_5)}$_2$] (0.9 mg, 0.0025 mmol) and the corresponding phosphite–nitrogen ligand (0.0055 mmol) in dichloromethane (0.5 mL) was stirred for 30 min. Subsequently, a solution of the corresponding substrate (0.5 mmol) in dichloromethane (1.5 mL) and benzylamine (131 µL, 1.5 mmol) were added. The reaction mixture was stirred at room temperature. After the desired reaction time, the reaction mixture was diluted with Et_2O (5 mL) and saturated NH_4Cl (aq) (25 mL) was added. The mixture was extracted with Et_2O (3×10 mL) and the extract dried over $MgSO_4$. Solvent was removed and conversion was measured by ^{1}H NMR spectroscopy. To determine the *ee* by HPLC (Chiralcel OJ, 13% 2-propanol/hexane, flow 0.5 mL min^{-1}), a sample was filtered over silica using 10% Et_2O/hexane mixture as the eluent.[38]

Acknowledgements

We thank the Spanish Government (Consolider-Ingenio CSD2006-0003, CTQ2007-62288/BQU, 2008PGIR/07 to O.P., and 2008PGIR/08 to M.D.), the Catalan Government (2005SGR007777), COST D40, Vetenskapsrådet (VR), and Astra Zeneca for their support.

[1] For reviews, see: a) J. Tsuji, *Palladium Reagents and Catalysis, Innovations in Organic Synthesis*, Wiley, New York, **1995**; b) B. M. Trost, D. L. van Vranken, *Chem. Rev.* **1996**, *96*, 395; c) M. Johannsen, K. A. Jorgensen, *Chem. Rev.* **1998**, *98*, 1689; d) A. ltz, M. Lautens in *Comprehensive Asymmetric Catalysis, Vol. 2* (Eds.: E. N. Jacobsen, A. Pfaltz, H. Yamamoto), Springer, Berlin, **1999**, Chapter 24; e) G. Helmchen, A. Pfaltz, *Acc. Chem. Res.* **2000**, *33*, 336; f) A. M. Masdeu-Bultó, M. Diéguez, E. Martín, M. Gómez, *Coord. Chem. Rev.* **2003**, *242*, 159; g) B. M. Trost, M. L. Crawley, *Chem. Rev.* **2003**, *103*, 2921; h) E. Martín, M. Diéguez, *C. R. Chim.* **2007**, *10*, 188; i) Z. Lu, S. Ma, *Angew. Chem.* **2008**, *120*, 264; *Angew. Chem. Int. Ed.* **2008**, *47*, 258.

[2] a) T. Hayashi, A. Yamamoto, T. Hagihara, Y. Ito, *Tetrahedron Lett.* **1986**, *27*, 191; b) T. Hayashi, *Pure Appl. Chem.* **1988**, *60*, 7; c) Recently this concept has also been used to explain the chiral induction by the Trost ligand, see: C. P. Butts, E. Filali, G. C. Lloyd-Jones, P. O. Norrby, D. A. Sale, Y. Schramm, *J. Am. Chem. Soc.* **2009**, *131*, 9945.

[3] See, for example: a) B. M. Trost, R. C. Bunt, *J. Am. Chem. Soc.* **1994**, *116*, 4089; b) B. M. Trost, A. C. Krueger, R. C. Bunt, J. Zambrano, *J. Am. Chem. Soc.* **1996**, *118*, 6520.

[4] See, for instance: a) G. J. Dawson, G. C. Frost, J. M. J. Williams, *Tetrahedron Lett.* **1993**, *34*, 3149; b) P. von Matt, A. Pfaltz, *Angew. Chem.* **1993**, *105*, 614; *Angew. Chem. Int. Ed. Engl.* **1993**, *32*, 566; c) P. Sennhenn, B. Gabler, G. Helmchen, *Tetrahedron Lett.* **1994**, *35*, 8595.

[5] The flexibility that the biaryl moiety offers can be used to fine-tune the chiral pocket formed upon complexation. See, for example: a) O. Pàmies, M. Diéguez, C. Claver, *J. Am. Chem. Soc.* **2005**, *127*, 3646; b) Y. Mata, M. Diéguez, O. Pàmies, C. Claver, *Adv. Synth. Catal.* **2005**, *347*, 1943.

[6] See, for instance: a) G. P. F. van Strijdonck, M. D. K. Boele, P. C. J. Kamer, J. G. de Vries, P. W. N. M. van Leeuwen, *Eur. J. Inorg. Chem.* **1999**, 1073; b) M. Diéguez, O. Pàmies, C. Claver, *Adv. Synth. Catal.* **2005**, *347*, 1257; c) M. Diéguez, O. Pàmies, C. Claver, *J. Org. Chem.* **2005**, *70*, 3363; d) M. Diéguez, O. Pàmies, C. Claver, *Adv. Synth. Catal.* **2007**, *349*, 836; e) O. Pàmies, M. Diéguez, *Chem. Eur. J.* **2008**, *14*, 944; f) E. Raluy, O. Pàmies, M. Diéguez, *J. Org. Chem.* **2007**, *72*, 2842.

[7] R. Prétôt, A. Pfaltz, *Angew. Chem.* **1998**, *110*, 337; *Angew. Chem. Int. Ed.* **1998**, *37*, 323.
[8] The choice of the oxazole and thiazole nitrogen donor units is based on the fact that they resemble the successful oxazoline unit but are much more robust.
[9] a) K. Kallstrom, C. Hedberg, P. Brandt, A. Bayer, P. G. Andersson, *J. Am. Chem. Soc.* **2004**, *126*, 14308; b) C. Hedberg, K. Kallstrom, P. Brandt, L. K. Hansen, P. G. Andersson, *J. Am. Chem. Soc.* **2006**, *128*, 2995.
[10] O. Pàmies, M. Diéguez, G. Net, A. Ruiz, C. Claver, *Organometallics* **2000**, *19*, 1488.
[11] Similar behavior has been observed for other phosphite–nitrogen ligands. See, for example: a) reference [4b]; b) M. Diéguez, O. Pàmies, *Chem. Eur. J.* **2008**, *14*, 3653.
[12] For more successful applications, see: a) P. Dierkes, S. Randechul, L. Barloy, A. De Cian, J. Fischer, P. C. J. Kamer, P. W. N. M. van Leeuwen, J. A. Osborn, *Angew. Chem.* **1998**, *110*, 3299; *Angew. Chem. Int. Ed.* **1998**, *37*, 3116; b) B. Wiene, G. Helmchen, *Tetrahedron Lett.* **1998**, *39*, 5727.
[13] G. Helmchen, S. Kudis, P. Sennhenn, H. Steinhagen, *Pure Appl. Chem.* **1997**, *69*, 513.
[14] See, for instance: a) A. Sudo, K. Saigo, *J. Org. Chem.* **1997**, *62*, 5508; b) G. J. Dawson, J. M. J. Williams, S. J. Coote, *Tetrahedron: Asymmetry* **1995**, *6*, 2535; c) C. J. Martin, D. J. Rawson, J. M. J. Williams, *Tetrahedron: Asymmetry* **1998**, *9*, 3723.
[15] For successful applications, see also: a) G. J. Dawson, J. M. J. Williams, S. J. Coote, *Tetrahedron Lett.* **1995**, *36*, 461; b) D. A. Evans, K. R. Campos, J. S. Tedrow, F. E. Michael, M. R. Gagné, *J. Am. Chem. Soc.* **2000**, *122*, 7905; c) D. Popa, C. Puigjaner, M. Gomez, J. Bene *t*Buchholz, A. Vidal-Ferran, M. A. Pericas, *Adv. Synth. Catal.* **2007**, 349, 2265.
[16] In contrast to Pd-catalytic systems, Ir, Ru, W, and Mo catalysts provide very high selectivity for the attack at the nonterminal carbon to give the chiral product. See, for instance: a) C. Bruneau, J. L. Renaud, B. Demersemen, *Chem. Eur. J.* **2006**, *12*, 5178; b) A. V. Malkov, L. Gouriou, G. C. Lloyd-Jones, I. Starý, V. Langer, P. Spoor, V. Vinader, P. Koèovský, *Chem. Eur. J.* **2006**, *12*, 6910; c) B. M. Trost, S. Hildbrand, K. Dogra, *J. Am. Chem. Soc.* **1999**, *121*, 10416; d) A. Alexakis, D. Polet, *Org. Lett.* **2004**, *6*, 3529; e) B. M. Trost, M. H. Hung, *J. Am. Chem. Soc.* **1983**, *105*, 7757; f) G. C. Lloyd-Jones, A. Pfaltz, *Angew. Chem.* **1995**, *107*, 534; *Angew. Chem. Int. Ed. Engl.* **1995**, *34*, 462.
[17] For recent successful applications of Pd catalysts, see: a) S.-L. You, X.-Z. Zhu, Y.-M. Luo, X.-L. Hou, L.-X. Dai, *J. Am. Chem. Soc.* **2001**, *123*, 7471; b) R. Hilgraf, A. Pfaltz, *Synlett* **1999**, 1814; c) R. Hilgraf, A. Pfaltz, *Adv. Synth. Catal.* **2005**, *347*, 61.
[18] a) S. Deerenberg, H. S. Schrekker, G. P. F. van Strijdonck, P. C. J. Kamer, P. W. N. M. van Leeuwen, J. Fraanje, K. Goubitz, *J. Org. Chem.* **2000**, *65*, 4810; b) F. Fernández, M. Gómez, S. Jansat, G. Muller, E. Martín, L. Flores Santos, P. X. García, A. Acosta, A. Aghmiz, M. Jiménez-Pedrós, A. M. Masdeu-Bultó, M. Diéguez, C. Claver, M. A. Maestro, *Organometallics* **2005**, *24*, 3946.
[19] The equilibrium between the two diastereoisomers takes place through the so-called apparent π-allyl rotation. This has been shown to occur through dissociation of one of the coordinated atoms of the bidentate ligand, which allows the ligand to rotate. See: A. Gogoll, J. Örnebro, H. Grennberg, J. E. Bäckvall, *J. Am. Chem. Soc.* **1994**, *116*, 3631.
[20] This study indicates that isomer **27A** reacts around 1.3 times faster than isomer **27B**.
[21] This is also consistent with the fact that for both isomers the most electrophilic allylic terminal carbon atom is the one *trans* to the phosphite in the major isomer **A**.
[22] The formation of compound **C** was confirmed by adding an excess of ligand, which resulted in an increase in the amount of species **C** present in solution.
[23] A. M. Porte, J. Reibenspies, K. Burgess, *J. Am. Chem. Soc.* **1998**, *120*, 9180.
[24] M. A. Pericàs, C. Puigjaner, A. Riera, A. Vidal-Ferran, M. Gómez, F. Jiménez, G. Muller, M. Rocamora, *Chem. Eur. J.* **2002**, *8*, 4164.
[25] This study indicates that isomer **34B** reacts around 1.5 times faster than isomer **34A**.
[26] G. J. H. Buisman, P. C. J. Kamer, P. W. N. M. van Leeuwen, *Tetrahedron: Asymmetry* **1993**, *4*, 1625.
[27] P. R. Auburn, P. B. Mackenzie, B. Bosnich, *J. Am. Chem. Soc.* **1985**, *107*, 2033.
[28] C. Jia, P. Müller, H. Mimoun, *J. Mol. Catal. A* **1995**, *101*, 127.
[29] J. Lehman, G. C. Lloyd-Jones, *Tetrahedron* **1995**, *51*, 8863.
[30] T. Hayashi, A. Yamamoto, Y. Ito, E. Nishioka, H. Miura, K. Yanagi, *J. Am. Chem. Soc.* **1989**, *111*, 6301.
[31] P. von Matt, G. C. Lloyd-Jones, A. B. E. Minidis, A. Pfaltz, L. Macko, M. Neuburger, M. Zehnder, H. Ruegger, P. S. Pregosin, *Helv. Chim. Acta* **1995**, *78*, 265.
[32] M. Kollmar, B. Goldfuss, M. Reggelin, F. Rominger, G. Helmchen, *Chem. Eur. J.* **2001**, *7*, 4913.
[33] B. M. Trost, P. E. Strege, L. Weber, *J. Am. Chem. Soc.* **1978**, *100*, 3407.
[34] Jaguar 4.2, Schrödinger, Inc. Portland, OR, **1991–2000**.
[35] a) A. D. Becke, *J. Chem. Phys.* **1993**, *98*, 5648; b) C. Lee, W. Yang, R. G. Parr, *Phys. Rev. B* **1988**, *37*, 785.
[36] P. J. Hay, W. R. Wadt, *J. Chem. Phys.* **1985**, *82*, 299.
[37] R. J. van Haaren, P. H. Keeven, L. A. van der Veen, K. Goubitz, G. P. F. van Strijdonck, H. Oevering, J. N. H. Reek, P. C. J. Kamer, P. W. N. M. van Leeuwen, *Inorg. Chim. Acta* **2002**, *327*, 108.
[38] O. Pàmies, G. P. F. van Strijdonck, M. Diéguez, S. Deerenberg, G. Net, A. Ruiz, C. Claver, P. C. J. Kamer, P. W. N. M. van Leeuwen, *J. Org. Chem.* **2001**, *66*, 8867.
[39] J. P. Janssen, G. Helmchen, *Tetrahedron Lett.* **1997**, *38*, 8025.

Received: July 3, 2009
Published online: November 20, 2009

